Criticality study of a spent fuel pool using SCALE 6.2.3 and MCNP6.2

Cheyeza Mulasi

orcid.org/0000-0001-7245-6320

Dissertation submitted for the degree *Magister Scientiae* in Nuclear Engineering at the North-West University

Supervisor: Prof V.V Naicker

Graduation:

Student number: 26047578

DECLARATION OF AUTHOR

I, Cheyeza Mulasi, declare that the work provided in the following dissertation is my own original work and has not previously been submitted by me for a degree at this or any other tertiary institution.

Signed:…….
Cheyeza Mulasi
Date:…….
North-West University, Potchefstroom

ACKNOWLEDGEMENTS

Firstly, I would like to thank God for the strength, ability, and opportunity to pursue and complete this qualification. My parents, Antoinette Ngodzweni, Dhuma Mulasi and Jake Mulasi for their constant support throughout my life and even in this study. My siblings Katlego, Khanyi, Khanyisa and Kirk for unknowingly pushing me when times were hard and lastly my extended family and friends. Notably Kutlwano for being my cheerleader *beke le beke.*

Thank you to my supervisor Professor Vishana Naicker for your patience and guidance. You pushed me even in moments when I did not believe I could finish.
To the SARChi Chair in Nuclear Engineering, thank you for supporting me financially throughout my master's programme.

ABSTRACT

The North-West University (NWU) through the Reactor Analysis group in UETS plans to conduct research on the spent fuel pool using capabilities of the in-house code, North-West University Reactor Code Suite (NWURCS). Due to the unavailability of specifications of the Koeberg reactor and spent fuel pool, open-source literature has been used with assumptions that enable the development of a methodology and data to be relevant to Koeberg.

This is the initial effort to perform spent fuel pool studies. The purpose of this study was to develop a methodology, which will guide further spent fuel pool studies and also verify the spent fuel pool modelling capabilities of NWURCS.

The study considered the burnup of a fuel assembly and criticality of the spent fuel pool. Furthermore, criticality was studied using the AP1000 Combined License Technical Report (COLA) spent fuel pool system as a reference. Due to the unavailability of boron information for the system, a boron concentration study was carried out to gain more insight into the simulation, since boron is a significant material in the spent fuel pool. Sensitivity studies were also carried out. The calculations showed that the model agree well with the results given in the COLA document. Furthermore, MCNP6 and KENO-VI calculations for the spent fuel pool showed good agreement between each other.

Keywords:

MCNP6.2, Spent fuel pool, Criticality, SCALE6.2.3, NEWT, NWURCS.

TABLE OF CONTENTS

DECLARATION OF AUTHOR ..... **I**

ACKNOWLEDGEMENTS ..... **II**

ABSTRACT ..... **III**

ABBREVIATIONS ..... **XI**

CHAPTER 1: INTRODUCTION **1**

1.1 Background **1**

1.2 Problem statement **4**

1.3 Research Aim and Objectives **5**

CHAPTER 2: LITERATURE REVIEW **7**

2.1 Cross section Processing (XSProc) **8**

2.2 NEW Transport **8**

2.2.1 The neutron transport equation 9

2.3 ORIGEN **12**

2.4 Fuel depletion and spent fuel. **13**

2.5 Monte Carlo Techniques **13**

2.5.1 Analogue simulation 13

2.5.2 Shannon entropy for the fission source distribution 15

2.5.3 Accuracy of the multiplication factor 16

2.5.4 Random numbers 16

2.6 Criticality studies of the spent fuel pool **16**

2.7 One group reactor equation **17**

CHAPTER 3 REACTOR AND SPENT FUEL POOL 18

3.1 The North Anna Reactor 18

3.1.1 Description 18

3.1.2 Fuel assembly and fuel pellet 19

3.1.3 Guide tubes and control rods 21

3.2 Spent fuel pool (SFP) 22

3.2.1 Description 22

3.2.2 Fuel arrangement and loading pattern. 28

CHAPTER 4 METHODOLOGY 31

4.1 NEWT 31

4.1.1 NEWT input file 31

4.1.2 Depletion in SCALE 33

4.2 Power profile and isotopic characterization 35

4.3 $kinf$ convergence 38

4.4 Introduction to spent fuel pool modelling 39

4.5 NWURCS modelling 40

4.6 MCNP6 41

4.6.1 MCNP6 input file 41

4.7 KENO-VI models 43

4.8 Boundary conditions 44

CHAPTER 5 RESULTS AND DISCUSSION 45

5.1 $kinf$ convergence 45

5.2 Burn-up model comparison 47

5.3 Model verification 53

5.3.1 Spent fuel pool 54

5.3.2 Material verification 55

5.3.3 Volume verification 57

5.4 Model analysis 58

5.4.1 Boron test 59

5.4.2 Spent fuel pool sensitivity analysis 62

CHAPTER 6 CONCLUSIONS AND RECOMMENDATIONS 66

6.1 Conclusions 66

6.2 Recommendations 67

6.2.1 Further Studies 67

6.2.2 NWURCS 68

BIBLIOGRAPHY 68

ANNEXURES 72

ANNEXURE 1 72

ANNEXURE 2 74

ANNEXURE 3 76

LIST OF TABLES

Table 1-1: North Anna power station vs Koeberg power station 4

Table 3-1: Properties of North Anna reactor (Thokwane, 2020)..... 18

Table 3-2: Fuel assembly properties (Thokwane, 2020)..... 21

Table 3-3: Properties of guide tubes (VEPCO, 2009) 22

Table 3-4: COLA spent fuel pool storage cell specifications..... 24

‘Table 4-1: NEWT input file description..... 31

Table 4-2: Nuclides from (Gauld, et al., 2011)..... 38

Table 4-4: $\boldsymbol{kinf}$ convergence..... 39

Table 5-1: Results for Local Grid Convergence Calculations. 45

Table 5-2: Power profile study..... 48

Table 5-3: Burnt SFP results 49

Table 5-4: burnt SFP for 5wt% and 1.6wt%..... 50

Table 5-5: Indicates all the cases and their respective change in $\boldsymbol{kinf}$ in pcm. 51

Table 5-6: Loaded SFP boron test..... 52

Table 5-7: Illustrate the Base Model Results 58

Table 5-8: $\boldsymbol{kinf}$ results for varied Boron concentrations for a 12 by 12 system..... 59

Table 5-9: pcm table for COLA vs modelled KENO-VI results..... 62

Table 5-10: Spent fuel pool sensitivity analysis..... 63

Table 5-11: Spent fuel pool sensitivity analysis of COLA sensitivity (Westinghouse Electric Company, 2006)..... 64

Table 5-12: Spent fuel pool sensitivity analysis of this study 64

Table 5-13: Delta comparison of COLA and KENO-VI..... 65

LIST OF FIGURES

Figure 2-1: Computational cell in ESC approach (Rearden & Jessee, 2018) 11

Figure 3-1: North Anna fuel assembly cross sectional view 20

Figure 3-2: North Anna fuel pellet 21

Figure 3-3: Guide tube without control rod cross-section 22

Figure 3-4: AP1000 spent fuel pool layout (Westinghouse Electric Company, 2006) 23

Figure 3-5: SPF axial view 25

Figure 3-6: Layout of one rack in region 2 26

Figure 3-7: In the side facing the wall canisters 27

Figure 3-8: Cross section of spent fuel pool 27

Figure 3-9: Canister development 28

Figure 3-10: Allowable fuel assembly arrangement in region 2 "1-out-of 4 5wt% fresh" storage 29

Figure 4-1: Relative isotopic importance in burnup credit criticality calculations 36

Figure 4-2: List of important nuclides based on SCALE 37

Figure 4-3: NWURCS nested structure 40

Figure 5-1: k-inf vs Number of local grids 46

Figure 5-2: Δk vs local grids 47

Figure 5-3: List of important nuclides based on SCALE 49

Figure 5-4: $\boldsymbol{kinf}$ vs boron for loaded spent fuel pool 53

Figure 5-5: Spent fuel pool region 2 layout 54

Figure 5-6: NWURCS material input 55

Figure 5-7: Cross section of spent fuel pool 56

Figure 5-8: Spent fuel pool side view 57

Figure 5-9: Boron test results 60

Figure 5-10: $\boldsymbol{kinf}$ vs boron concentration 61

ABBREVIATIONS

cdf's	Cumulative distribution function
Cm	Centimetres
COLA	AP1000 Combined License Technical Report
DMRE	Department of Mineral Resources and Energy
EOC	End of cycle
ESC	Extended Step Characterization
EPR	European Pressurized Reactor
FA	Fuel assembly
IAEA	Internal Atomic Energy Agency
IRP	Integrated Resource Plan (IRP).
LCG	Linear Congruential Generator
MCNP	Monte Carlo N-particle
NDP	National Development plan
NEWT	New Transport algorithm
NPP	Nuclear Power Plant
NWU	North-West University
NWURCS	North-West University Reactor Code Suite
ORIGEN	Oak Ridge Isotope GENeration
pdf's	Probability distribution functions
PWR	Pressurized water reactor
RFI	Request for Information
SFP	Spent fuel pool
SMR	Small modular reactor

TRITON	The Transport Rigor Implemented with Time-depended Operation for Neutronic depletion
UETS	Unit for Energy and Technology Systems

CHAPTER 1: INTRODUCTION

1.1 Background

South Africa's national development plan (NDP) 2030 offers a long-term plan for the country. The NDP proposes that South Africa will have an energy sector that provides reliable and efficient energy services at competitive rates by the year 2030. The government seeks to address the electricity needs of the country over a period of 20 years (2010-2030) through the Integrated Resource Plan (IRP). The IRP is an electricity infrastructure development plan which is developed based on the most cost-effective supply and demand while ensuring resource security and that it is environmentally viable. This IRP was updated and is presently available as the IRP 2019 (DMRE, 2019).

In its quest to mix the energy grid and compensate the ending of the design life of the Koeberg power station, the South African government has indicated in the 2019 IRP that the country will invest in smaller nuclear units on the basis that they are manageable.

In June of 2020, the South African government issued a Request for Information (RFI). The purpose for the RFI is to collect technical and financial information from different Nuclear Power Plant (NPP) vendors to revive the nuclear build programme in the country. The main aspects to be considered for the nuclear programme are: NPP technologies; license ability of plant design in South Africa; plant design features and construction feasibility. (Department of Minerals Resource and Energy, 2020). The RFI envisages the total power to be 2500MW. The department is considering Pressurized Water Reactors (PWRs) and Small Modular Reactors (SMRs). Many developing countries have been doing research on SMRs due the high capital costs of large power reactors (World Nuclear Association, n.d.).

With the growing interest in cleaner and greener energy, nuclear energy is still, without a doubt, an option for many countries. Nuclear energy is the world's second largest source of low-carbon power with a total contribution of 28% in 2017 (World Nuclear Association, 2020). Even with the mixed emotions regarding nuclear energy, countries continue to operate and invest in new nuclear builds. Developing countries have started to show an interest in nuclear power and introducing it into their energy grid.

Nuclear power is the production of electricity through energy that is produced during fission reactions. Fission occurs when neutrons are emitted by fissionable nuclei. These neutrons then induce fissions in other fissile and fissionable nuclei. This reaction continues and can be quantified using the multiplication factor (k) (Lamarsh & Baratta, 2001). The multiplication factor can be

denoted as the ratio of the number of fissions in one generation to the number of fissions in the preceding generation. When the number of fissions increases with time, $k > 1$ and the system is considered supercritical, if the number of fissions decreases with time, $k < 1$, and the system is considered subcritical. However, when the chain reaction is constant, $k = 1$, and the system is considered critical. Most nuclear reactors use ceramic pellets containing enriched Uranium-235 inside the fuel rods (Ganguly, 2001). Uranium is not a highly radioactive substance in its natural state and can be handled without high-end shielding equipment. When the enriched uranium atom is split, it produces fission products, which are radioactive. This fuel, once it is removed from the reactor and can no longer be used as nuclear fuel or be reprocessed, can be classified as nuclear waste.

Nuclear waste generates a substantial amount of heat, hence the need to store it in wet storage. Nuclear waste can be categorized into three main levels which are distinguished by the amount of radioactivity per unit volume (Rosenfeld & Feng, 2011). These are low level waste, intermediate level waste and high-level waste. Low level waste is radioactive waste that emits less than 4GBq/t of alpha activity or 12GBq/t of beta gamma activity. This type of waste has little effects on the environment and humans. Intermediate waste is more radioactive than low level waste, however the decay heat generated is still quite low. High level waste on the other hand is highly radioactive and produces a significant amount of decay heat in the first few years after being removed from the reactor.

Fission creates fission products from the fuel which includes Uranium-235 and plutonium isotopes. These fission products account for most of the heat and the high hazardous radiation in high level waste.

High level waste requires more sophisticated storage compared to the other two types of waste. High level waste needs to be stored in wet storage until it is cool enough to be moved to dry storage should it not be reprocessed.

A spent fuel pool (SFP) is a cooling facility which stores depleted fuel assemblies (FA) that have been removed from the reactor core. The SFP stores FA under about 1.82 m of water which assists with cooling of the fuel assemblies (NRC, 2017).

Since the operation of the very first commercial nuclear power plant over 60 years ago, the number of accidents associated with nuclear power is less compared to accidents associated with other energy sources (World Nuclear Association, n.d.). This number continues to decrease as advancements are made to existing nuclear power plant designs and precautions are made from

studying previous accidents. The Fukushima Daiichi nuclear accident in 2011, one of the two level seven accidents in nuclear history according to the International Atomic Energy Agency (IAEA, n.d.), is currently the only known accident that has affected the spent fuel pool. The spent fuel pool stores high-level radioactive waste for several years before it can be removed and taken to medium term storage or more permanent storage.

The spent fuel pools use simple and non-complex systems to avoid accidents (de la Rosa Blul, et al., 2018). The Fukushima Daiichi accident in 2011 in Japan highlighted the possible potential weaknesses of nuclear plants and their ability to withstand extreme scenarios which may not have been studied in the design process (National Nuclear Regulator, 2017). International nuclear regulators have warned nuclear power plant operating countries to have highly effective and responsive mitigation strategies for the spent fuel pool, regardless of the frequency and unlikelihood of spent fuel pool accidents (Nuclear Regulatory Commission, 2014).

Part of this strategy will require appropriate computational models. In the context of South Africa, the NWU has established capabilities in reactor analysis, and these capabilities need to be extended to the spent fuel pool studies. To start this process, the depletion model of the fuel assembly was developed using SCALE, a computer system used for many radiation transport applications. The Transport Rigor Implemented with Time-depended Operation for Neutronic depletion (TRITON) is a SCALE control module that allows 2-D and 3-D depletion calculations to be performed by coordinating iterative calls between cross-section processing codes and a neutron transport solver. New Transport algorithm (NEWT) is the transport solver, a neutronic code that has many uses such as calculation of 2-D eigenvalues, forward and adjoint flux solutions, multigroup flux spectrum calculations, and cross section collapse calculations. NEWT is part of the SCALE software package and is used together with XSProc and ORIGEN for flux and depletion calculation. The depleted number densities calculated using the TRITON module will be used to define the FAs that will be modelled in the SFP.

The North Anna reactor in the United States of America is similar to the Koeberg reactor in South Africa. It is on this basis that the results can be useful in the context of Koeberg. Therefore, the Safety Analysis Report of the North Anna Reactor was used as the specification document to build the fuel assembly model. Table 1-1 below shows some of the similar parameters between North Anna and Koeberg power stations (Bredell & Stott, n.d.), (The Virtual Nuclear Tourist, n.d.) and (Nyalunga, et al., 2016)

Table 1-1: North Anna power station vs Koeberg power station

Parameter	North Anna	Koeberg
Thermal power	2942.2 MWt	
Net Capacity (MWe)		1860 MWe
Moderator	H_2O (stated as a PWR)	H_2O (stated as a PWR)
Coolant,	H_2O	H_2O
Number of fuel assemblies	157	157
Fuel assembly layout	17 x 17	17 x 17
Fuel Type	UO_2	UO_2
No of loops	3	3
Core inlet T	563.0 K	549.8K
Core Outlet T	601.7 K	583.2K

However, the spent fuel pool specifications for both reactors are not available. A Westinghouse AP1000 standard COLA technical report was found and was used as a reference in order to model the spent fuel pool in the study.

1.2 Problem statement

South Africa has been operating a nuclear plant for just under 40 years. Previous studies at the North-West University have focused on the methodology for fuel assembly and full core calculations. This was carried out to promote research in nuclear energy given the presence of nuclear reactors in South Africa. However, a study on the criticality of the spent fuel pool has not been carried out since research in this area also requires attention. In this study the methodology will be developed. Technical details about the Koeberg reactors and the spent fuel pools are classified. Therefore, in order to develop a methodology, the North Anna reactor will be used to develop the fuel assembly models. This is because the North Anna reactor and the Koeberg reactors are very similar in design. For the purpose of the spent fuel pool analysis, information from articles on other spent fuel pools are used. Obtaining more applicable results is subject to the availability of accurate information from the relevant regulatory body or the plant operator.

Currently, the methodology based on existing modelling developed at the NWU needs to be extended for the study of a SPF.

1.3 Research Aim and Objectives

The aim of this research project was to establish a methodology at the North-West University (NWU) in which the multiplication factor of the spent fuel pool containing spent fuel assemblies can be calculated.

The objectives of this study are as follows:

- To simulate the burnup of fuel assemblies using computer software and perform isotopic characterisation of the fuel assemblies;
- To build MCNP6/KENO-VI spent fuel pool simulation models and perform calculations using isotopic data from burnt fuel assembly simulations;
- To modify the spent fuel pool model to build a base model documented in the reference literature; and
- To perform a series of sensitivity and verification tests on the spent fuel pool models.

1.4 Report outline

Chapter 1 Introduction: This chapter provides an overview of the current state of the nuclear industry in South Africa. It also gives a background on the nuclear plans within government over the past 10 years.

Chapter 2 Literature Review: This chapter provides a literature overview of the principles of reactor physics that govern the codes and methodology.

Chapter 3 Reactor and Spent Fuel Pool: This chapter gives the description of the reactor and the spent fuel pool used for the models.

Chapter 4 Methodology: This chapter gives a detailed overview on the steps taken to obtain results. It also indicates some of the assumptions made for the purpose of this study.

Chapter 5 Results and Discussions: This chapter contains the results obtained from studying the isotopes of the fuel removed from the reactor core and loaded in the spent fuel pool and criticality studies in the spent fuel pool.

Chapter 6 Conclusions: This chapter contains conclusions made from studying the results obtained and providing recommendations based on those conclusions.

Chapter 7 References: This chapter contains the references used in this study.

CHAPTER 2: LITERATURE REVIEW

Chapter overview

This chapter provides the literature overview of the principles of reactor physics that govern the process followed in this study. It provides discussion on the step characterization method in NEWT, the neutron transport equations and fuel depletion. Included is the theory on the software used and how they are applied in the methodology.

The burnup calculations are called by TRITON (T-NEWT), which is a control module used in SCALE. The SCALE Code System is a modelling and simulation suite for nuclear safety analysis and design. This includes lattice and reactor physics, and sensitivity and uncertainty analysis. It is developed, maintained, tested, and managed by the Reactor and Nuclear Systems Division (RNSD) of Oak Ridge National Laboratory (ORNL) (Rearden & Jessee, 2018).
The flow of the calculations in TRITON follows a structure that links one component to the next component of SCALE. These components are XSProc, NEWT and ORIGEN.

TRITON is used to calculate number densities and fluxes at the end of a fuel cycle (EOC). This is carried out as follows. The number densities at the beginning of cycle (BOC) are known. The first code called is XSProc which produces the collapsed cross section data set. This multigroup data is supplied to NEWT, NEWT then calculates the fluxes in the different regions, so that the burnup can be calculated in the different regions. ORIGEN utilizes these fluxes provided by NEWT and calculates the number densities from the previous known point (initially it will be $t = 0$) to the next point using the depletion Equation 9. These number densities are then used as the starting point for the next cycle, and the calculation chain is then repeated for the next cycle. The cycles continue until the last cycle. The final isotopic data set is then available for use in the spent fuel pool.

The second component is the calculation of the multiplication factor for a newly loaded spent fuel pool, without subsequent decay calculations. For this calculation MCNP6.2 is used, together with KENO-VI and NWURCS. NWURCS is used to generate input files for KENO-VI and MCNP6. Input files for a section of the spent fuel pool is generated using NWURCS, then KENO-VI and MCNP calculations are performed. KENO-VI calculations are carried out because the open-source document used for reference in this study provides KENO-VI results.

2.1 Cross section Processing (XSProc)

The XSProc module was designed for the treatment of self-shielding and cross-section temperature correction (Rearden & Jessee, 2018). XSProc is used by the criticality safety analysis sequence to calculate k_{eff} or k_{inf} of a three-dimensional (3-D) system model using the multigroup computation mode, which employs XSProc to process cross sections for temperature corrections and problem-dependent resonance self-shielding.

The standard composition data and other engineering-type specifications, such as volume fraction or percent theoretical density, temperature, and isotope distribution, as well as the unit cell data, are read by XSProc. Then, using XSProc, number densities and related data are generated, as well as geometry data for resonance self-shielding and flux-weighting cell calculations (Rearden & Jessee, 2018).

XSProc first calls BONAMI or CENTRM to calculate the flux. The code then calls PMC to calculate the collapsed cross sections using the microscopic cross sections supplied to BONAMI or CENTRM and the fluxes by BONAMI or CENTRM. These collapsed cross sections are also known as self-shielded cross sections or group constants. In the applications used in this work, 256 groups were generated (Rearden & Jessee, 2018).

2.2 NEW Transport

The NEWT (NEW Transport algorithm) code is part of the SCALE package, and it is a multi-group discrete ordinates neutral particle transport code with flexible meshing capabilities. This code employs the Extended Step Characteristic spatial discretization approach using arbitrary polygonal mesh cells (Kim & DeHart, 2010). The ESC (Extended Step Characterization) approach is based on two crucial assumptions which are: all properties within each cell are uniform and cell boundaries are defined by straight lines (Rearden & Jessee, 2018). As a lattice physics code, NEWT can calculate weighted multi-group cross sections and spatial fluxes. NEWT produces a simpler version of complex problems, where regions are derived based on the global NEWT grid and are homogenized.

2.2.1 The neutron transport equation

Neutron transport theory deals with the transportation of neutrons through different media. Neutrons are neutral particles, and it is assumed that they travel in straight lines until they collide with a nucleus where they can be absorbed or scattered into a new direction (Hummel & Novog, 2011).

The neutron transport equation is a neutron conservation equation. NEWT uses deterministic methods to numerically solve this equation. The transport equation may be written in many forms based on the application. In lattice physics calculations, it can be written in terms of the angular neutron flux as the dependent variable. The neutron angular flux is the product of angular neutron density and neutron velocity (Stacey, 2007).

The time independent form of the linear transport equation is expressed as:

$$\hat{\Omega} \cdot \vec{\nabla} \cdot \psi(\vec{r}, \hat{\Omega}, E) + \Sigma_t(\vec{r}, E)\psi(\vec{r}, \hat{\Omega}, E) = Q(\vec{r}, \hat{\Omega}, E) \quad (1)$$

Where:

$\psi(\vec{r}, \hat{\Omega}, E)$ is the angular flux at position $\vec{r}$ per unit volume in direction $\hat{\Omega}$ per unit solid angle at energy E per unit energy;

$\Sigma_t(\vec{r}, E)$ *is* total macroscopic cross-section at position $\vec{r}$ and energy E; and

Q is the source at position $\vec{r}$ per unit volume in direction $\hat{\Omega}$ per unit solid angle at energy E per unit energy.

The source Q is composed of three terms:

1. The scattering source

$$S(\vec{r}, \hat{\Omega}, E) = \int_{4\pi} d\hat{\Omega}' \int_0^{\infty} dE' \Sigma_s(\vec{r}, \hat{\Omega}' \rightarrow \hat{\Omega}, E' \rightarrow E)\psi(\vec{r}, \hat{\Omega}, E'), \quad (2)$$

where:

$\Sigma_s(\vec{r}\hat{\Omega}' \rightarrow \hat{\Omega}, E' \rightarrow E) \equiv$ macroscopic scattering cross section at position $\vec{r}$ from initial energy E' and direction $\hat{\Omega}'$ to final energy E and direction $\hat{\Omega}$.

2. The fission source

$$F(\vec{r}, \hat{\Omega}, E) = \chi(\vec{r}, E) \int_0^\infty dE' \nu(\vec{r}, E') \Sigma_f(\vec{r}, E') \psi(\vec{r}, \hat{\Omega}, E') \quad (3)$$

where:

$\Sigma_f(\vec{r}, E) \equiv$ macroscopic fission cross section at position $\vec{r}$ and energy E' (assumed to be isotropic)

$\nu(\vec{r}, E') \equiv$ number of neutrons released per fission event at position $\vec{r}$ and energy E';

$\chi(\vec{r}, E) \equiv$ fraction of neutrons that are born at $\vec{r}$ and at energy E.

3. External or fixed source

$$S(\vec{r}, E) \quad (4)$$

Due to the difficulty that can arise in solving the transport equation, numerical approximations are made (Rearden & Jessee, 2018). If we consider shapes such as cylinders, it is difficult to effectively model such a shape on a 2-D cartesian coordinate system. In such instances it is more effective to divide the cylinder into rectangular cells which will give an acceptable approximation. The smaller the rectangular cells, the more accurate the approximation.

NEWT Step characterization

In addition to the above-mentioned, it is also difficult to apply discrete-ordinates methods particularly when solving complicated non-orthogonal geometries due to the nature of finite difference approximations for spatial derivatives. The method of characteristics can be used to solve the transport equation analytically along characteristic direction within a computational cell. The angular flux ψ is solved along the characteristic directions (Rearden & Jessee, 2018). The streaming term of the transport equation can then be written as follows:

$$\hat{\Omega} \cdot \vec{\nabla} \psi(\vec{r}, \hat{\Omega}, E) = \frac{d\psi(s, E)}{ds} \quad (5)$$

When the energy variable E in the above equation is omitted (as in a multigroup formalism), the equation can therefore be written as:

$$\frac{d\psi(s)}{ds} + \sigma_t(s)\psi(s) = Q(s) \tag{6}$$

s is the distance along the characteristic direction $\hat{\Omega}$. The solution of Equation 6 becomes:

$$\psi(s) = \psi_0 e^{-\sigma_t s} + e^{-\sigma_t s} \int_0^s Q e^{-\sigma_t s'} ds' \tag{7}$$

where ψ_0 is the known angular flux at $s = 0$. Boundary conditions of known cell sides are used to obtain the values of ψ_0 . The equation above is then used to compute the angular fluxes of the unknown sides. In the step characteristic method, the source Q, and the macroscopic total cross section σ_t are assumed constant within the boundaries of the computational cell and the angular flux is assumed constant on the cell boundaries of the incoming direction. The integration of the above equation produces Equation 8.

$$\psi(s) = \psi_0 e^{-\sigma_t s} + \frac{Q}{\sigma_t}(1 - e^{-\sigma_t s}) \tag{8}$$

Figure 2-1 gives a visual representation of a computational cell in the application of the step characterization approach.

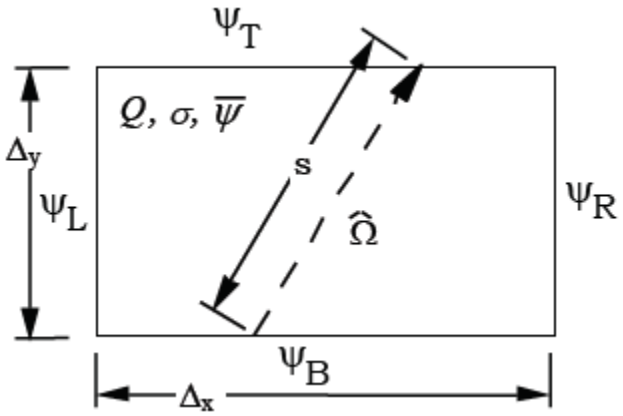

Figure 2-1: Computational cell in ESC approach (Rearden & Jessee, 2018)

This figure can be interpreted as follows: Assume the characteristic direction is shown by $\hat{\Omega}$. The unknown side of the angular flux can be written in terms of the average flux of the known sides. For the characteristic direction $\hat{\Omega}$, the top flux Ψ_T is the unknown side and can be computed

according to the average contributions from the known sides Ψ_B and Ψ_L. The known fluxes of the two sides are taken to be constant along the length of each side to represent the average angular flux in the direction $\widehat{\Omega}$ where they must be obtained from an external boundary condition or in an adjacent cell calculation.

2.3 ORIGEN

The Oak Ridge Isotope GENeration (ORIGEN) is a solver of the set of ordinary differential equations that describe nuclide generation, depletion, and decay.

$$\frac{dN_t}{dt} = \sum_{j \neq i} (l_{ij}\lambda_j + f_{ij}\sigma_j)N_j(t) - (\lambda_i + \sigma_i\phi)N_i(t) + S_i(t) \quad (9)$$

Where:

$N_i = number\ of\ nuclide\ i$

$\lambda_i = decay\ constant\ of\ nuclide\ i$

$l_{ij} = fractional\ yield\ of\ nuclide\ i\ from\ nuclide\ j\ decay$

$\sigma_i = spectrum - averaged\ removal\ cross\ section\ for\ i$

$f_{ij} = fractional\ yield\ of\ nuclide\ i\ from\ removal\ of\ nuclide\ j$

$\phi = neutron\ flux$

$S_i = source$

The above equation is not spatially dependent and thus can be solved at a moment in space or the spatial average over a chosen volume. When the spatial average interpretation is used for the neutron flux the energy dependence of the appropriate cross section is grouped as an average flux-weighted cross sections σ_t . The equation above can then be written as a matrix as follows:

$$\frac{d\vec{N}}{dt} = A\vec{N}(t) + \vec{S}(t) \quad (10)$$

In the equation above, A refers to the transition matrix which can be described as $A = A_\sigma\phi + A_\lambda$ where A_σ contains the reaction terms and A_λ is part of the decay terms.

Alpha, beta, neutron, and gamma emission spectra can be considered by ORIGEN during decay.

2.4 Fuel depletion and spent fuel

Fuel depletion refers to the long-term changes in the properties of a nuclear reactor fuel element over its lifetime. These are determined by the changes in the composition resulting from fuel burnup and how they are compensated (Stacey, 2007). Power generating reactors are subjected to significant isotopic changes which occur over a period of hours to years.
During operation, the changes in composition occur by different mechanisms. One mechanism is transmutation. It is the conversion of a chemical element from one element to another. Transmutation by decay occurs by emission of an alpha or beta particle.

2.5 Monte Carlo Techniques

The Monte Carlo based code MCNP6 can be used to calculate the multiplication factor, neutron flux, fission energy and heating energy deposition in the fuel assemblies from fission. The Monte Carlo method is extremely effective for problems with complex geometries where calculations of integral quantities such as the neutron multiplication eigenvalue factor is desired (Boston, 2014)
In this study, MCNP6 is used to calculate the multiplication factor for a given part of a spent fuel pool configuration. The Monte Carlo N-particle Transport (MCNP) code uses the stochastic approach. Stochastic methods or Monte Carlo simulation do not solve the transport equation as in the deterministic method-based codes. This approach simulates particle transport for each particle by tracking the path of each individual particle throughout its lifetime and records (tallies) the average behaviour of these particles (Boston, 2014). The code deals with transport of neutrons, gamma rays, and coupled transport, such as the transportation of secondary gamma rays due to neutron interactions. The MCNP code can also treat the transport of electrons, both primary source electrons and secondary electrons created in gamma-ray interactions (Shultis & Faw, n.d.).

2.5.1 Analogue simulation

The analogue simulation traces the path of a neutron as it moves through matter. The source of neutrons is predominantly from the fission source. The fission source has a distribution in space, energy and direction that can be considered to be isotropic. Probability distribution functions (pdfs) and cumulative distribution function (cdfs) can be used to characterize these distributions. In three dimensions, when three random numbers are generated and the cdf for the spatial fission distribution is selected, the location in space is defined. When another number is generated, and the cdf for the fission spectrum is used, the energy of the source particle is determined. The direction of the neutron source is defined when third and fourth numbers are generated with the

cdfs for the independent angular variables. When the neutron is released, it travels in a straight line until it experiences a collision (Stacey, 2007). The probability that a neutron experiences collision at a distance in that straight line is given as Equation 11:

$$T(s) = \Sigma_t(s) exp\left[-\int_0^s \Sigma_t(s')ds'\right] \quad (11)$$

Which is the pdf for the collision distance *s*. Selecting another random number will then give the positions at which the collision will occur.

It is next needed establish the type of nuclide and the type of reactions taking place. Therefore, the composition at the time of the collision must be known. Equation 12 gives an indication of the probability for the reaction *x* of a neutron to interact with an isotope of species *i*:

$$P_{ix} = \frac{N_i \sigma_{ix}}{\Sigma_{i,x} N_i \sigma_{ix}} \quad (12)$$

Where N_i is the number density of nuclide *i* in the region, σ_{ix} is the microscopic cross section for reaction *x* for nuclide *i* at the energy of the neutron.

When the reaction type is absorption, the history of the neutron is terminated while the energy and the location of the absorbed neutron are recorded, and a new history begins. However, if the reaction is elastic scattering, a new random number is created and equated to the cdf for the cosine of the scattering angle in the centre of mass co-ordinates (CM) to obtain μ_{cm}. It is to be noted that in the CM co-ordinate system, the scattering is usually isotropic. The energy of the scattered neutron is uniquely associated to μ_{cm} from scattering kinematics for energies above thermal. This is illustrated by Equation 13.

$$\mu = cos\theta = \frac{1}{2}(A+1)\sqrt{\frac{E}{E'}} + \frac{1}{2}(A-1)\sqrt{\frac{E'}{E}} \quad (13)$$

Another random number is created and equated to the appropriate cdf when it is inelastic scattering or elastic scattering of thermal neutrons.

After the scattering event has been characterized, the neutron is treated as if it were a fission source neutron, and the calculation is repeated until the neutron is absorbed or it leaks from the system. KENO-VI, which is a part of the SCALE 6.2.3 package, is also a Monte Carlo code, and follows a similar process as outlined above for MCNP6.

2.5.2 Shannon entropy for the fission source distribution

In order to obtain correct results (for example the multiplication factor) that are not affected by the initial guess for the fission source distribution, the fission source must be converged. Ideally, this means that source points must be located at every volume where fission is possible for a given cycle.

In practice, the initial source distribution guess is made for iteration 1. Thereafter, the neutrons that arise from the fission process become the source neutrons for the next iteration (cycle), as explained in Section 2.5.1. This process repeats for each cycle. The source distribution therefore spreads out as the cycles progress. This spreading out of the source is monitored in terms of the Shannon entropy. The Shannon entropy H_{src} is a concept in which a single number H_{src} is calculated for each cycle to assist in characterizing the convergence of the distribution of the fission source.

In order to calculate H_{src}, a 3D grid needs to be superimposed on the fissile and fissionable areas. MCNP6 will automatically determine such a grid that encloses all fission sites for a cycle (Los Alamos National Laboratory, 2017).

The Shannon entropy of the discretized source distribution is given by Equation 14.

$$H_{src} = -\sum_{J=1}^{N} P_J \cdot ln_2(P_J) \quad (14)$$

N is the number of grid boxes in the superimposed mesh and P_j is the number of source sites in the J-th grid box over the total number of source sites.
H_{src} varies between 0 for a point distribution to $ln_2(N)$ for a uniform distribution (Brown, 2006). For each cycle of a criticality calculation, MCNP6 computes and provides H_{src}.
The first cycle when H_{src} falls within one standard deviation of its average for the last half of cycles up to that point will be reported by the code, along with a recommendation to reject at least

that many cycles (which are then called inactive). H_{src} vs. cycle plots should be inspected to confirm the number of idle cycles (also called inactive or skipped cycles) required for convergence. If the number of inactive cycles is less than that recommended, then the calculation must be re-started, with the recommended (or larger) number of inactive cycles.

The average value of H_{src} for the latter half of the active cycles, as well as its standard deviation (also referred as the population) will be computed using MCNP6.

Users must examine the convergence of the fission source distribution while doing criticality calculations using the Shannon entropy function within MCNP6. The output of the calculations will be incorrect if H_{src} is not converged prior to starting the active cycles. KENO-VI also has Shannon entropy fission source convergence diagnostic capabilities.

2.5.3 Accuracy of the multiplication factor

When the fission source is converged, a calculation with more active cycles (for example 100) will produce a more accurate value for *k* compared to a calculation with fewer active cycle (for example 20). This is because the standard deviation with more active cycles has a smaller standard deviation compared to the calculation with fewer active cycles.

2.5.4 Random numbers

Random number generation is crucial for Monte Carlo calculations. There are several algorithms for random number generation that exist. Section 2.5.1 discussed how random numbers are used. MCNP6 uses the linear congruential generator (LCG). The LCG is a method for calculating a sequence of pseudo-random numbers using a discontinuous piecewise linear equation.
This generator stores the most recent value and allows one to generate the exact same sequence again and again. By utilizing the same numbers repeatedly, the variety of differences that changing numbers would create is reduced. Any changes in the comparisons are thus related to variations in the models themselves (Sigman, n.d.).

2.6 Criticality studies of the spent fuel pool

The actinides produced from transmutation decay of fuel isotopes and the fission products account for most of the radioactive waste produced in nuclear reactors as discussed in Chapter One. At shutdown, fission products are major contributors of reactivity. However, due to the comparatively short half-life, the reactivity decreases noticeably after being removed from the reactor. As

mentioned in Section 1.1, when removed from the reactor core, the actinides need to be stored for at least five years in the spent fuel pool. (IAEA, 2003)
The spent fuel pool provides safe storage for fresh fuel and spent fuel. The spent fuel pool contains water to a depth of about 1.82 m. This water is borated and provides sufficient shielding for operational staff during normal operation, and reduces radioactive gases released in an accident (Westinghouse Electric Company, 2006).

As the water in the pool continues to perform the above-mentioned functions, it is important to add more water into the pool as some of the water evaporates continuously from the heat.

Furthermore, nuclear criticality safety analysis must be carried out on the spent fuel pool system. Nuclear criticality safety analysis is of vital significance as it ensures the safety margin for the storage, transportation, reprocessing, and disposition of spent fuel assemblies.
The specific geometry and material composition for the spent fuel pool as used in this study is given in Section 3.2.1.

2.7 One group reactor equation

The one group reactor equation is defined as the birth rate divided by the leakage rate plus the absorption rate of neutrons, given in Equation 15. Although not implemented in the codes used in this study, it is helpful when it comes to interpreting criticality results, since one can infer trends in *k* using this equation (Stacey, 2007).

$$\mathbf{k = \frac{\upsilon \Sigma_f \phi}{DB^2 \phi + \Sigma_a \phi} = \frac{\upsilon \Sigma_f}{DB^2 + \Sigma_a}} \qquad \mathbf{(16)}$$

Consider boron for example. Boron in water is used as a neutron absorber material. Boron has a high absorption cross section for thermal neutrons and therefore assists in reducing and controlling the rate of fission. This characteristic of boron contributes to the absorption rate. The numerator of the equation defines the birth rate of the neutrons, while the denominator defines the sum of the leakage and absorption rate. Thus, when the boron concentration increases, the absorption rate increases, thus increasing the denominator and reducing the *k* value.

CHAPTER 3 REACTOR AND SPENT FUEL POOL

Chapter overview

This chapter provides detailed descriptions of the reactor and the spent fuel pool modelled in this study. It is noted that in terms of the reactor, only the fuel assembly was modelled for the burnup study to generate the isotopic characterisation to be used in the spent fuel calculation. The reactor was the North Anna reactor, and the spent fuel pool was the Westinghouse AP1000 spent fuel pool.

3.1 The North Anna Reactor

3.1.1 Description

The reactor chosen for the purpose of this study is the North Anna reactor. The North Anna reactor is a PWR and is similar to the Koeberg reactors. A previous neutronic reactor core study has already been conducted on this system at the NWU. The codes used were DRAGON and DONJON (Thokwane, 2020). Table 3-1 shows the fundamental properties of the North Anna reactor.

Table 3-1: Properties of North Anna reactor (Thokwane, 2020)

Properties	Values
Thermal power	2775 MWth
Pressure	15.513 MPa
Mass flow rate	3282.1 kg/m^{2}s
Inlet temperature	559.15 K
Outlet temperature	596.37 K

The North Anna Power Station comprises of two pressurized water reactors with a total electrical capacity of 1,806 MW. The plant is owned by Virginia Electric and Power Co. and Old Dominion Electric Cooperative. Unit 1 of the North Anna reactor commenced operation in 1978 with a license expiration date set for 2038 and unit 2 commencing in 1980 with a set license expiration date for 2040, (NEI & Dominion, 2008).

These reactors are based on a Westinghouse pressurized light water reactor design connected to a Westinghouse 3-loop nuclear steam supply system housed in a steel-lined, reinforced-concrete containment building (Thokwane, 2020).

Three fuel enrichments are used in the initial core loading. In the outer region of the core, fuel assemblies with the highest enrichments are placed, while the two lower fuel enrichments are arranged in a pattern in the inner and central region. About one-third of the fuel is removed and fresh fuel is loaded into the core at 18-month intervals, (VEPCO, 2009). The fuel remaining in the core is re-arranged to achieve optimum power distribution.

3.1.2 Fuel assembly and fuel pellet

The fuel assembly structure consists of a bottom nozzle, a top nozzle, guide and instrument thimbles, and grid structures. The top nozzle assists with attaching the guide thimble and provides flow area for the coolant leaving the fuel assembly. The bottom nozzle is a stainless-steel structure that enables the guide thimble locations to be connected to the internal interface of the reactor internals (VEPCO, 2009). Figure 3-1 shows the cross-sectional view of the fuel assembly. The fuel assembly has a 17 x 17 layout. The guide tubes and the instrumentation pin “look” the same due to the absence of control rods in the model.

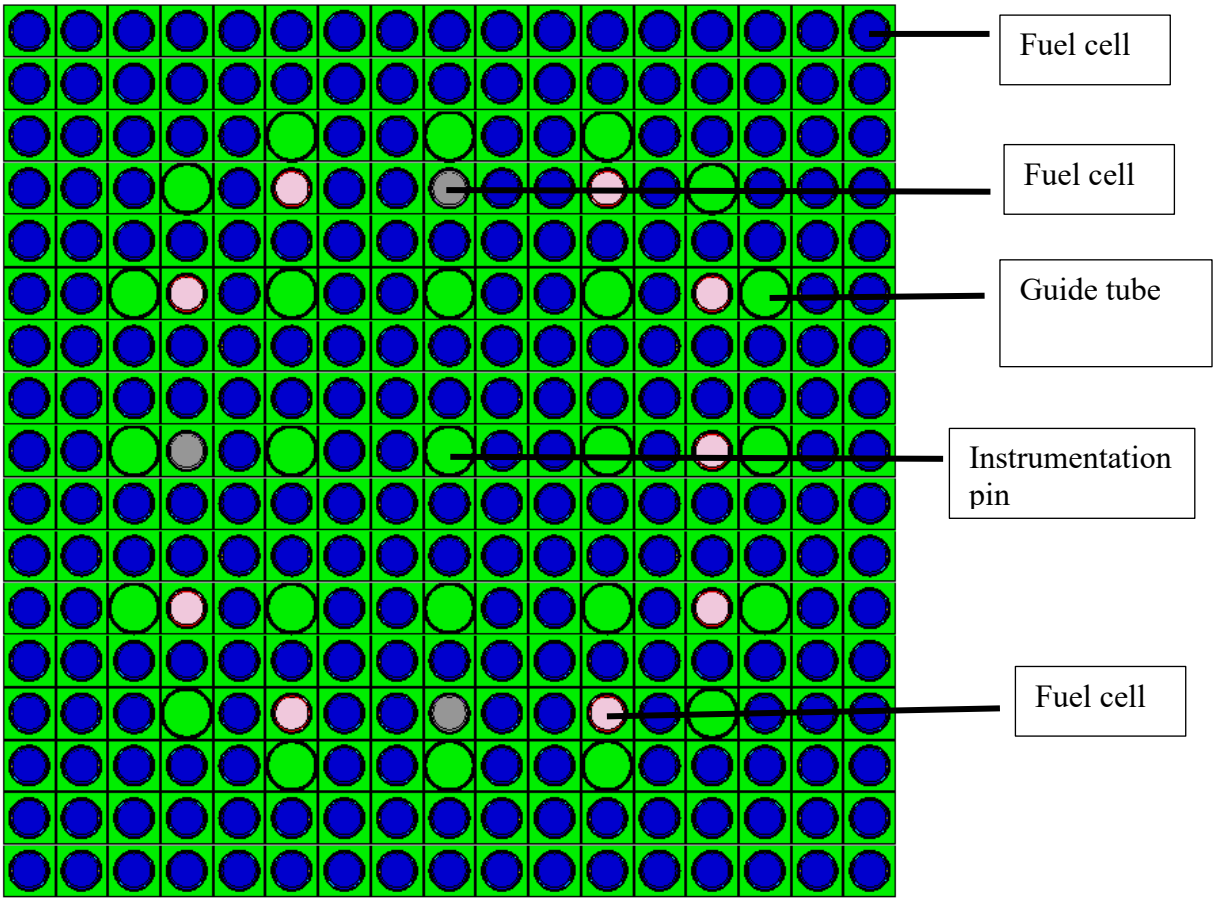

Figure 3-1: North Anna fuel assembly cross sectional view

For this study, it was assumed that the fuel assemblies are without spacer grids in order to keep the model simple. A previous study carried out by (G.P. Nyalunga, 2019) has shown that for a VVER system, there is a significant change in the multiplication factor when considering spacer grids. However, in terms of the objectives of the current study and to simplify the model, it was decided that the methodology development can be carried out without spacer grids being modelled, and the spacer grids can be incorporated in later studies. The value for k in the spent fuel pool, should the spacer grids be included, will change.

The North Anna fuel pellets are encircled with zircaloy cladding and moderator as shown in Figure 3-2 below. Table 3-2 shows the fuel assembly properties for the North Anna reactor. A gap is present between the cladding and the fuel pellet, which is not shown in the figure.

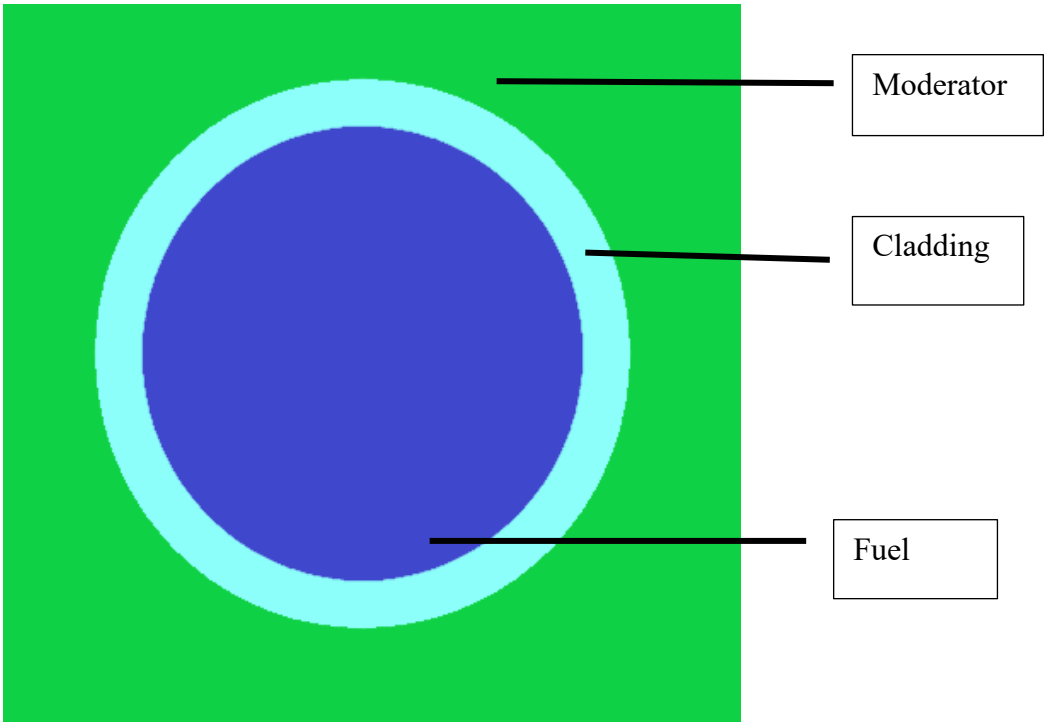

Figure 3-2: North Anna fuel pellet

Table 3-2: Fuel assembly properties (Thokwane, 2020)

Name	**Detail**
Number of fuel assemblies	157
Guide tube per FA	24
Instrumental pins per FA	1
Fuel enrichments	2.1%wt
	2.6wt%
	3.1wt%

3.1.3 Guide tubes and control rods

The fuel assemblies have 24 guide tubes. Figure 3-3 shows the properties of the guide tubes in the North Anna reactor. Guide tubes are a structural component made from zircaloy-4 that allow the insertion of control rods. The control rods in the North Anna reactor have neutron absorbers made from a silver-indium-cadmium alloy and are used to control the fission reactions in the reactor. The control rods were not modelled in this study due to the complexity of control rod modelling and that only a single FA was being modelled for this study. Hence, it was decided that the control

rods will not be modelled, since there are fuel assemblies present in the core at specific positions in which there are no control rods present.

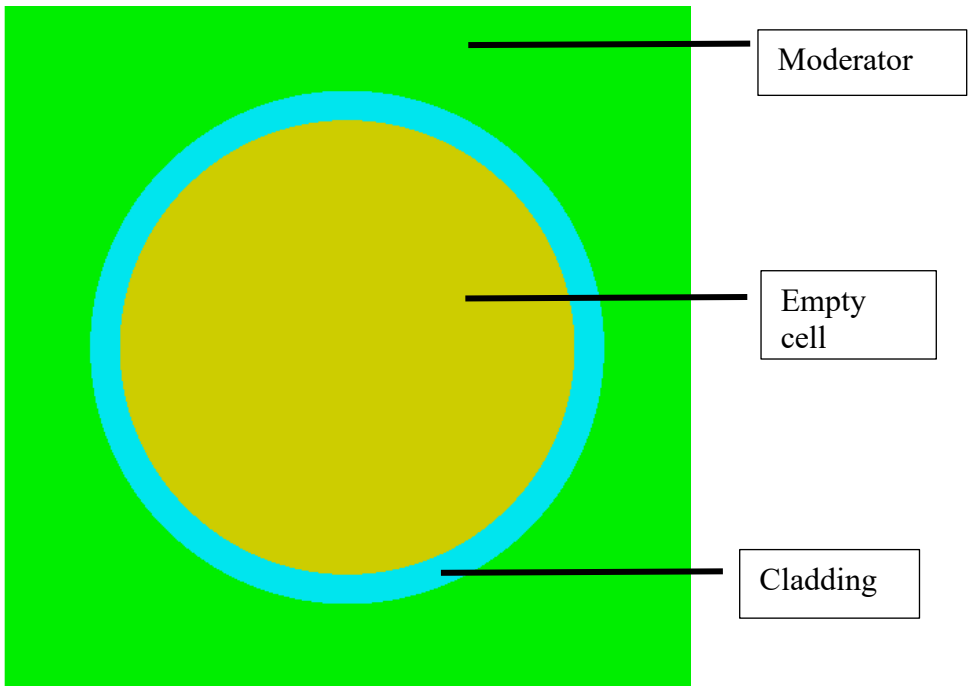

Figure 3-3: Guide tube without control rod cross-section

Table 3-3: Properties of guide tubes (VEPCO, 2009)

Property	**Value**
Temperature	500 K
Inner diameter	0.57150 cm
Outer diameter	0.61214 cm
Material density	6.55 g/cm^3

3.2 Spent fuel pool (SFP)

3.2.1 Description

The process of designing a SFP needs to consider relevant methods which include computational methods. With soluble boron credit (i.e., considering the boron in the water for the calculation), the maximum k_{eff} value must be less than 0.95, including all biases and uncertainties (Westinghouse Electric Company, 2006). Without boron in the water, this value should be less than 1.0. Therefore, these values must be maintained throughout the system in all circumstances.

For reasons stipulated in Section 1.1, the model used in this study was based on the AP1000 reactor and the storage capabilities of the spent fuel pool has 889 fuel assembly locations. These locations are divided into regions as shown in Figure 3-4. The dimensions for regions 1 and 2 are listed in Table 3-4.

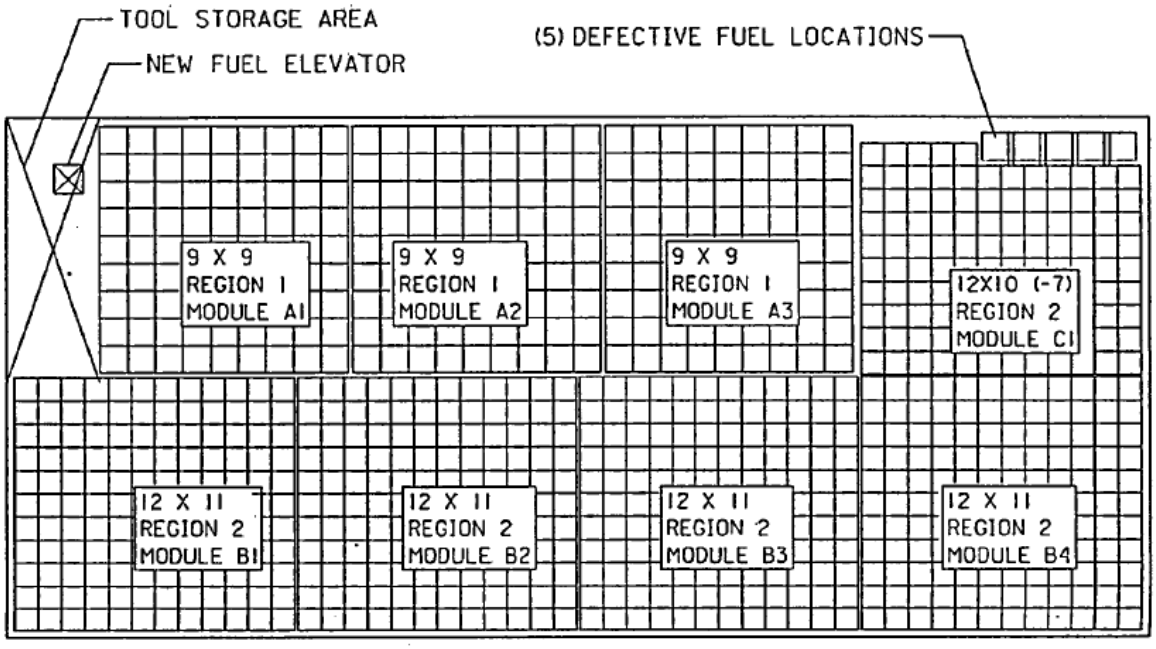

Figure 3-4: AP1000 spent fuel pool layout (Westinghouse Electric Company, 2006)

Table 3-4: COLA spent fuel pool storage cell specifications

Regions	Parameter	Value (cm)
Region 1	Storage cell centre-to-centre	27.686
	Storage cell width	22.352
	Storage cell length New fuel storage	506.73 491.49
	Storage cell wall thickness	0.1905
	Rack male pedestal	11.43
	Rack female pedestal	50.8 x 50.8 x 5.715
	Rack bearing pad	3.81
	Rack baseplate thickness	1.905
Region 2	Storage cell centre-to-centre	22.93112
	Storage cell width	22.352
	Storage cell length	506.73
	Storage cell wall thickness	0.1905
	Rack baseplate thickness	1.905

There are racks in each region. Region 1 consists of three racks, region 2 contains five racks and five individual defective fuel assembly storage cells. Each rack contains an array of storage cells. For example, the array for the racks in region 1 are 9 x 9.
To summarize, each region contains several racks and each rack contains an array of storage cells.

Region 1 has fewer racks compared to region 2 as shown above in Figure 3-4. The racks in region 2 have an array of 12 x 11 or 12 x 10. The storage cells of region 2 are smaller than those of region 1. The centre-to-centre pitch of the cells for region 1 is 27.686 cm while those cells of region 2 have a centre-to-centre pitch of 22.93112 cm.

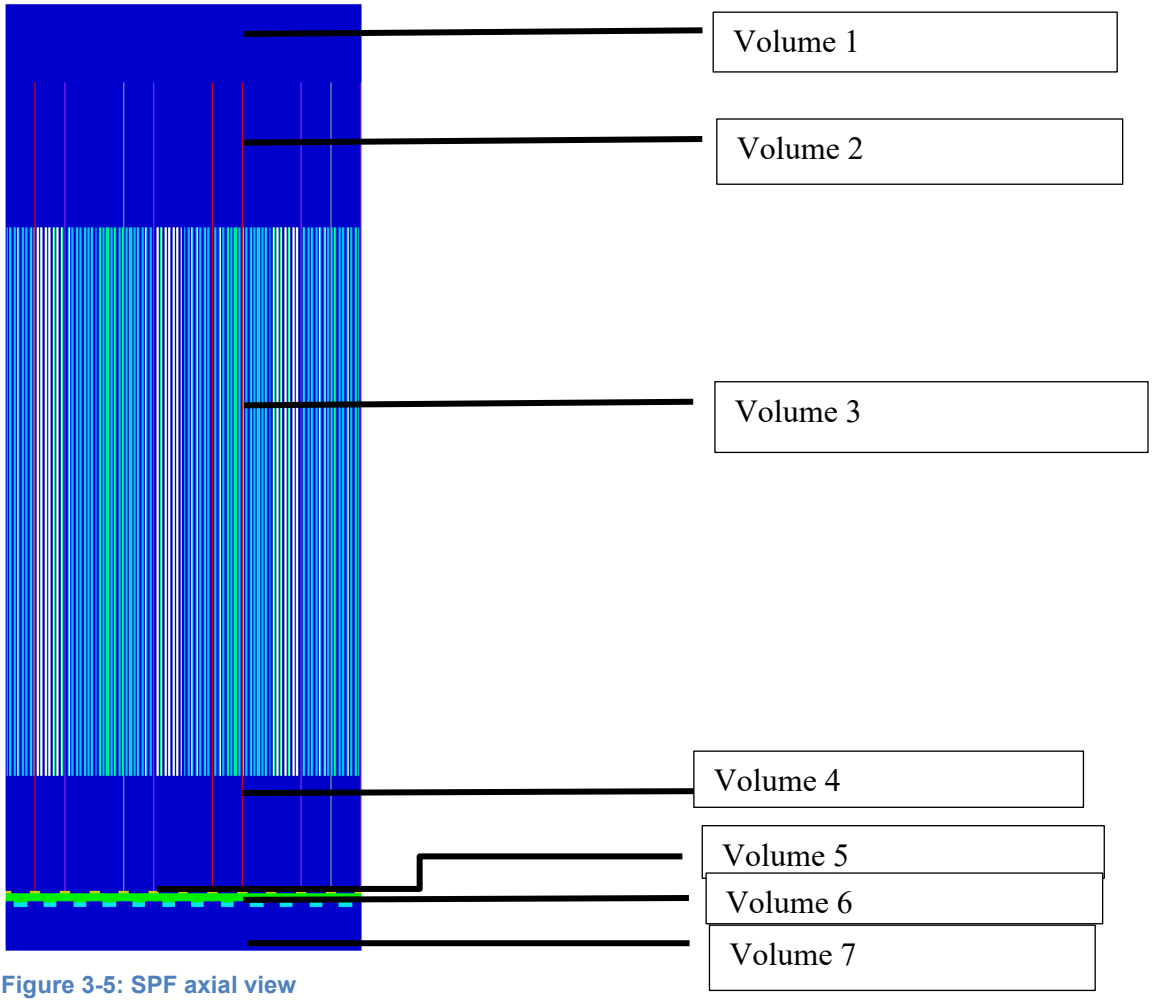

Figure 3-5: SPF axial view

To simplify the modelling process, the different components of a cell were split axially into prospective sections. The total length of the storage cell is 506.73 cm. At the bottom is the concrete floor (volume 7), which is followed by the pedestals (volume 6) as shown in Figure 3-5. The baseplate is elevated above the pedestals (shown as volume 5) and is followed by the bottom part of the stainless-steel canisters (this is volume 4). The active length of the fuel assembly is modelled inside the stainless-steel canisters (volume 3). These stainless steel cannisters are continued from volume 4. This is then followed by the top section of the stainless steel cannisters (volume 2) and finally the water reflector above the storage cell (volume 1).

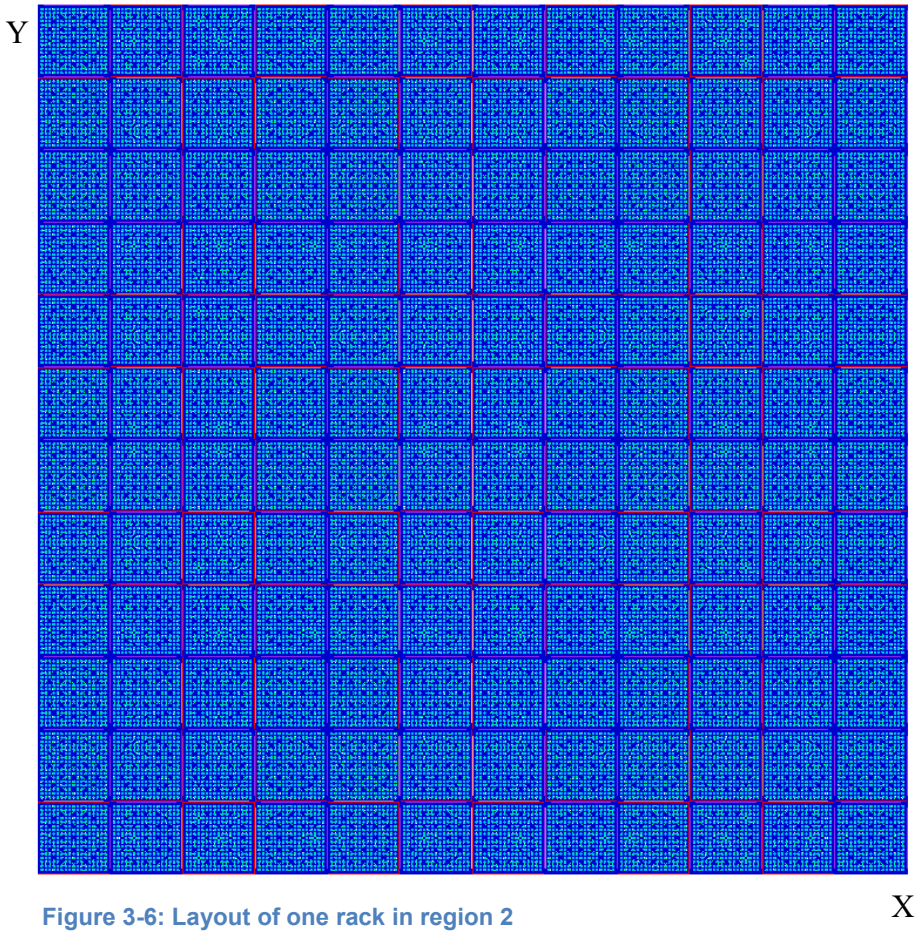

Figure 3-6: Layout of one rack in region 2

The fuel assembly is positioned inside the stainless-steel canister with an inside dimension of 22.352 cm and 0.1905 cm thickness. Attached to the stainless-steel canister are the Metamic panels which are 19.05 cm wide and have a thickness of 0.26924 cm. The Metamic panels function as the neutron absorber in the spent fuel pool and are held together by sheathing panels made from stainless steel with a thickness of 0.0889 cm. The Metamic panels and the sheathings panels are separated by a small gap modelled to be a void with a thickness of 0.03048 cm. The Metamic panels (together with the stainless steel cannister) span volumes 2, 3 and 4 shown in Figure 3-5. Figure 3-6 shows the x-y view of one of the racks of the SFP region 2. This figure shows a 12 x 12 rack, since this was the definition of one of the models that was used in this study. The racks shown in region 2 of Figure 3-4 are 12 x 11. Figure 3-7 shows four storage cells next to the outer wall. One can use the red “square lines” in the figures to identify Figure 3-7 in Figure 3-6.

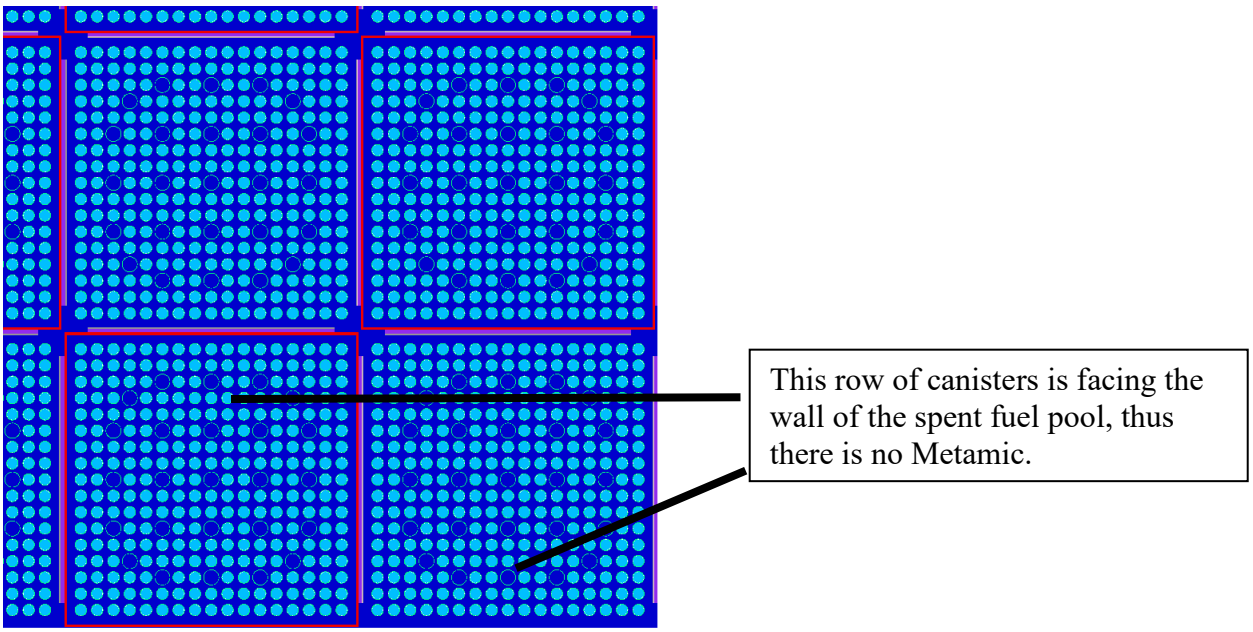

Figure 3-7: In the side facing the wall canisters

The detail where four storage cells in a rack meet are shown in Figure 3-8 This figure highlights the position of Metamic, void and sheathing panels.

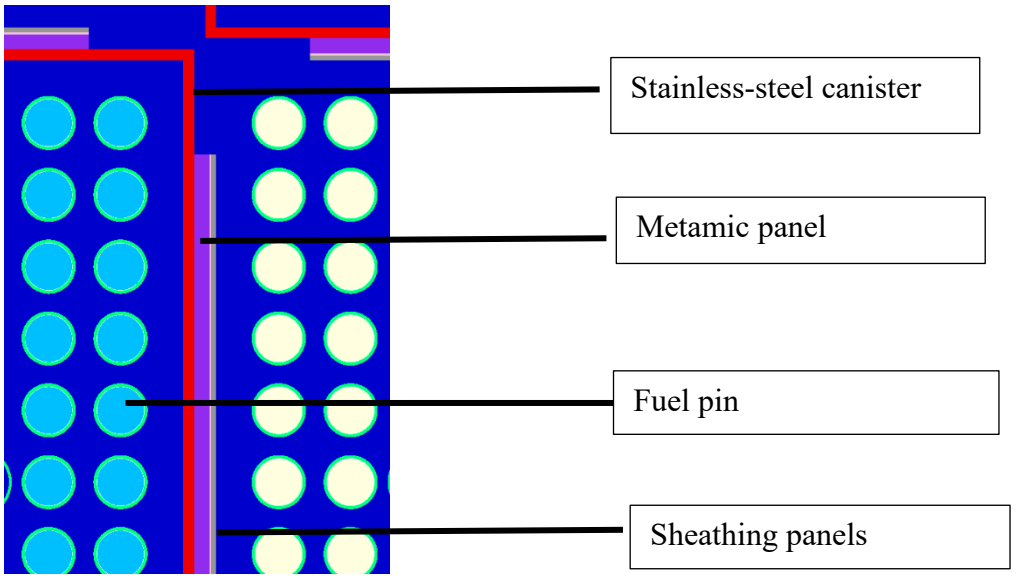

Figure 3-8: Cross section of spent fuel pool

The storage cells in the racks of Region 2 are formed through welding of open stainless canisters and are made of a combination of individual canister storage cells. To develop the storage racks

in region 2, four canisters are welded at the corners of each canister which then produces a further single storage cell at the centre of the four canisters. This can be seen in Figure 3-9 below. The "W" canisters are those that are welded at the corners in order to produce the "developed" canister.

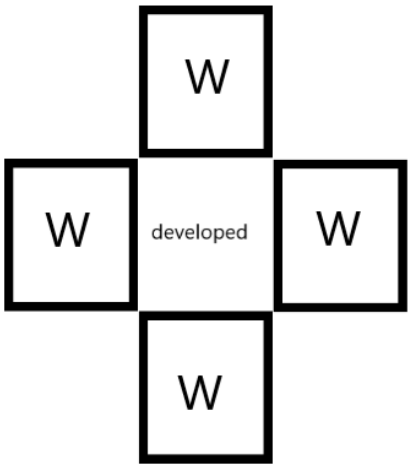

Figure 3-9: Canister development

The Metamic panels are affixed to the exterior surfaces of each stainless-steel canister, except for the surfaces which are indirectly facing the walls of the spent fuel pool.

3.2.2 Fuel arrangement and loading pattern

The general principle for spent fuel loading is arranging fuel assemblies in the storage racks in a in a way that always ensures subcriticality in the spent fuel pool. The licensing for spent fuel operation in the United States of America requires license holders to arrange fuel assemblies into the racks in a 1x4 pattern.

For the purpose of consistency due to the lack of data on North Anna spent fuel pool, the fuel loading pattern in this study follows the Westinghouse AP1000 17 x 17 spent fuel pool. Figure 3-10 shows the fuel arrangement used.

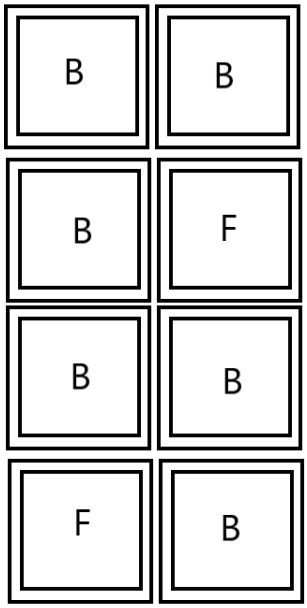

Figure 3-10: Allowable fuel assembly arrangement in region 2 "1-out-of 4 5wt% fresh" storage

The “B” in the arrangement represents depleted fuel assemblies or empty cells while the “F” represents fresh fuel assemblies with an initial enrichment that is equal or less than 5.0wt% U-235. However, depleted fuel can also be stored at “F” positions. This arrangement is a repeating array in the spent fuel pool which should not be changed. This repeating array is used to control the k_{eff} to ensure less burnup credit is required (Dominion Nuclear Connecticut, Inc , 2012).

It should be noted that the spent fuel pool design for the AP1000 might be different from that of the spent fuel pool for the North Anna fuel assemblies or the Koeberg fuel assemblies.

Although the fuel assemblies have the same dimensions in the radial plane, they have different lengths in the axial directions. The AP1000 fuel assemblies are longer than the North Anna and Koeberg fuel assemblies. This therefore means that the metamic plates together with the steel cannisters might be shorter in the North Anna or Koeberg spent fuel pool nodes.

However, since the burnup of spent fuel assemblies have maximum limits due to fuel performance considerations, it is most likely that the spent fuel designs would not differ drastically. Therefore, the NWURCS model should not change significantly. Also, the nested level approach used in NWURCS would also allow the changing of dimensions and materials to be carried out with relative ease.

Given that the present study is to develop methodology so that further research can be carried out, revision of the model will be required so that the Koeberg facility can be modelled. This will be carried out in later studies.

CHAPTER 4 METHODOLOGY

Chapter overview

This chapter describes the methods used to perform burnup and subsequent modelling of the burnt isotopes inventory in the spent fuel pool. This chapter also provides an outline on the research methods taken to build the spent fuel pool model as well as detailed description of the steps taken to perform sensitivity studies and the verification test on the models built.

4.1 NEWT

4.1.1 NEWT input file

The NEWT input is free form and keyword based. It is similar to many input files used in the Scale package. Data was supplied using data blocks which are defined as follows:
Read keyword [data] end keyword

The "read" commands are only terminated by the "end keyword", thus the data supplied can be written in different forms. Any row that is started with a (') is treated as a comment which is not be used in calculation. Further specifications and parameters can be defined within each data block.

The 'Table **4-1** shows the keyword name(s) and a description of each keyword of each data block (Rearden & Jessee, 2018).

'Table 4-1: NEWT input file description

Block type	**Recognized keywords**	**Description**
*Problem control parameters	parameter, parameters, param, parm, para	The parameters block is optional however it should follow the title card when used.
Material properties	material, materials, matl	This data block assign material characteristics for each material identity.

*Broad group collapse	collapse, coll	Defines broad group energy ranges to be created from the original group library when performing cross-section collapsing calculation
Simple-body geometry	geometry, geom	This data block defines the basic grid structure and all bodies placed within this grid structure.
*Boundary conditions	bounds, bnds	Defines boundary conditions which are to be applied on outer boundaries of the global unit.
Array specification	Array	Defines composition of all the unit placements within array. The units placed in the array block must be defined in the geometry block.
*Homogenization instructions	Homog, hmog, homo	Defines mixtures to be weighted by flux and homogenized for homogenized cross-section library
*Assembly discontinuity factors	Adf	Assigns type and location of planes at which assembly discontinuity factors are calculated.
*Flux plane	Flux	Provides allowance for x- or y- axis line definition in order to average and print computed fluxes.
*Mixing table	mixtable, mixt	Mixing table specifications.
Source definition	Src, source	Describes particle source strength for use in source calculations

(*) indicates optional data blocks.

In NEWT, a fuel assembly model was developed by specifying the fuel assembly's material composition such as number densities and temperature, and the geometry. Below is an example of a data block (Material) within a NEWT input file.

Read material

Mix=1 Pn=2 com=' water end

Mix=2 Pn=1 com=' 2.1 enriched fuel end

End material

Where:

M= mixture ID.

N=P_n order for scattering in mixture M

Com=' comment

Example of material command

```
read materials

 mix=4   pn=1  com="helium gap" end
 mix=3   pn=2  com="water" end
 mix=2   pn=1  com="cladding" end
 mix=1   pn=1  com="2.1 wt % enriched fuel " end
end materials
```

4.1.2 Depletion in SCALE

The main function of the depletion data block is that it specifies the material(m) in which to perform depletion calculations and specifies the basis to which the model power is normalized. However, it is also used to specify the ORIGENS solver and the ORIGENS depletion mode for each material and to include any optional instructions which are related to depletion.

Read depletion

$$m_1 \ m_2 \ m_3 \dots \dots \dots m_n$$

End depletion

Example of a depletion command

Read depletion

1 end

End depletion

In the example above, material 1 is to be burnt which indicates that material 1 is fuel.

The input format to perform burn-up includes the following mandatory data blocks (Rearden & Jessee, 2018):

a. Burndata

The burn data block specifies the power and depletion intervals required for depletion. These must be written in chronological order within the block. Below is an example for an acceptable format for SCALE.

Read Burndata

Power= p burn= B down= D nlib=N

End

Example of a Burndata command

```
read burndata
 power=10.20240  burn=45.65625  down=0 nlib=4   end
 power=10.20240  burn=45.65625  down=0 nlib=4   end
 power=10.20240  burn=91.3125   down=0 nlib=4   end
end burndata
```

P(MW/MTHM) is the average specific power, B (days) indicates the depletion interval length, D (days) is the length of decay interval and N is the number of depletion subintervals. Temporal discretization can be achieved by refining the number of depletion subintervals. This produces more cross sections and transport calculations per depletion interval.

b. Opus

OPUS is not mandatory, however it allows extraction of specific data from the ORIGEN output libraries, unit conversions and generate data to be plotted. TRITON uses the opus block by default; however, it only extracts default nuclides concentrations with a default unit.

Read opus

Units= gram

Symnuc= u-235 xe-131 pu-138 u-234 pu-239

Mat=1

End opus

Example of an opus command block

```
read opus
units=gram
symnuc=
    u-235 pu-239 u-238 pu-240 pu-241 sm-149 nd-143 Rh-103
    sm-151 Am-241 Xe-131 u-236 cs-133 gd-155 Np-237 sm-152
    Tc-99 nd-145 eu-153 pu-242 sm-147 Mo-95 pu-238 sm-150
    Ag-109 Ru-101 pd-105 Pr-141 Am-243 Eu-151  u-234
    pb-206 pb-207 pb-208 end
    matl=0 1  end
end opus
```

4.2 Power profile and isotopic characterization

When the FA leaves the core, after 4.5 years, the researchers assumed that the enrichment has decreased to about 1.6wt%. This is very crudely justified by the starting enrichments, 3.1wt%, 2.6wt%, and 2.1wt% for the fuel assemblies. These three enrichments are present so that the fresh core will have fuel enrichments close to that of a core that has already been operating for a few cycles. In this case, the 3.1wt% fuel assemblies will be those of the fresh fuel that will be loaded at later cycles, the 2.6wt% fuel assemblies loaded in the first core will be close to that of fuel assemblies of initial enrichment 3.1wt% but has been in the reactor core for 18 months, and with a resulting enrichment of around 2.6wt%. Similarly, a fuel assembly loaded in the fresh core with 2.1wt% would be close to that of a fuel assembly in later cycles that would have been in the core for two fuel reloading. The enrichments for the fresh core have a difference of 0.5%. It was therefore assumed that the burnt fuel assembly (after 4.5 years in the core) would have an enrichment corresponding to that of the 2.1wt% fuel assembly after it has been in the core for 18 months. Without performing any burnup calculations, it can be assumed that the enrichment can be approximated to 1.6wt% when spent. An alternate strategy could have been to calculate the burnup to a specified value. However, using the current strategy, it was simpler to carry out the sensitivity studies in terms of the number densities of the burnt isotopes.

In the NEWT/ORIGEN burnup calculations, it is then assumed that the number density of U-235 will be approximately 1.6wt% at the end of burnup. This then allows one to adjust the power for the calculation so that the end burn up will be 1.6wt%. In terms of the axial direction (which is the vertical direction, also referred to as the z direction), a constant power was used. It is then assumed

that the core burns uniformly in the z (axial) direction, and only a single calculation is required. Since the main objective of this study is to develop a methodology the uniform distribution assumption was used to set up the calculation chain. More appropriate power profiles should be considered in later studies.

Studies have been carried out to identify the important nuclides in spent fuel pool analysis. This study will perform calculations using these nuclides identified (Gauld, et al., 2011). These are listed in Table 4-2. The actinides and fission products which are deemed to have the highest influence on the neutron multiplication factor in the spent fuel pool are shown in the graph below. These actinides are crucial for burnup and criticality. Due to the short half-life of Xe-131, it is not always considered for burn-up credit but shown in the table (Gauld, et al., 2011).

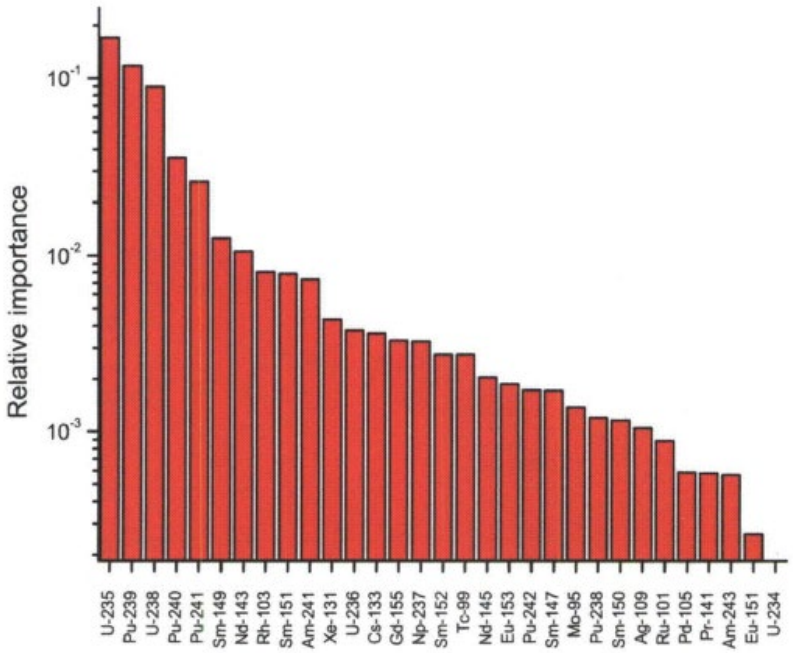

Figure 4-1: Relative isotopic importance in burnup credit criticality calculations

Two models were carried out. One with Opus and the other without Opus. The Opus model specifies the isotopes that should be given in the output, these isotopes are those shown in Figure 5-3. The model without using Opus gives an output of default isotopes from SCALE.

```
read opus
  units=atom
  volume=1
  symnuc=
    u-234   u-235   u-236   u-238   pu-238  pu-239  pu-240
    pu-241  pu-242  pu-243  ag-107  ag-109  am-241  am-242
    am-243  cd-106  cd-108  cd-110  cd-111  cd-112  cd-113
    cd-114  cd-116  cm-242  cm-243  cm-244  cm-245  cs-133
    cs-134  cs-135  cs-137  eu-153  eu-154  eu-155  gd-154
    gd-155  in-113  in-115  mo-95   np-237  nd-143  nd-144
    nd-145  nd-146  nd-148  nd-150  np-237  o-16    pb-206
    pb-207  pb-208  pd-105  pm-147  pr-141  rh-103  ru-101
    sm-147  sm-148  sm-149  sm-150  sm-151  sm-152  sm-154
    tc-99   xe-131
            end
  matl=0 1  end
end opus
```

Figure 4-2: List of important nuclides based on SCALE

Table 4-2: Nuclides from (Gauld, et al., 2011)

Identified Nuclides		Default from SCALE	
u-235	nd-145	u-234	mo-95
pu-239	eu-153	u-234	tc-99
u-238	pu-242	u-236	ru-101
pu-240	sm-147	u-238	rh-103
pu-241	mo-95	pu-238	ag-109
sm-149	pu-238	pu-239	cs-133
nd-143	sm-150	pu-240	nd-143
rh-103	ag-109	pu-241	nd-145
sm-151	ru-101	pu-242	sm-147
am-241	pd-105	pu-243	sm-149
xe-131	pr-141	am-241	sm-150
u-236	am-243	am-242m	sm-151
cs-133	eu-151	am-243	sm-152
gd-155	u-234	cm-242	eu-153
np-237	pb-206	cm-243	gd-155
sm-152	pb-207	cm-244	o-16
tc-99	pb-208	cm-245	

4.3 k_{inf} convergence

Convergence calculations assessing the input parameters for the fuel assembly calculations produces more refined results of k_{inf}. In this study, the parameters considered were the local and global grids in the fuel assembly. It is assumed that the fuel assembly has no gaps and hence no spacer grids in between as was discussed in section 3.1.2 .

Table 4-3 below show the combinations of grids that were studied for the convergence of k-inf.

Table 4-3: k_{inf} convergence

Global unit	Local unit
64	4
64	8
64	12
64	16
64	20
64	24
64	28
64	32
64	36
64	40

4.4 Introduction to spent fuel pool modelling

It is important to note that the long-term goals of research under which this study falls is to model the Koeberg Spent Fuel System in South Africa. The Koeberg Reactor System is very close to that of the North Anna specifications. The Safety Analysis Report of the North Anna Reactor is available in the open literature (VEPCO, 2009), and therefore information regarding the fuel assemblies in terms of geometry and material composition is available. However, due to the propriety nature and unavailability of information of the Koeberg or North Anna spent fuel pool, the spent fuel pool in this study was modelled using the COLA specifications because this information is available in open literature.

It is to be noted that the COLA document contains results which could be used to verify the modelling methodology being developed in this study. However, the fuel assemblies defined in the North Anna Safety Analysis Report and the COLA document differ in the active length of the fuel assembly, being 364.99 cm and 426.72 cm respectively.

4.5 NWURCS modelling

NWURCS is a code wrapper that is currently being developed by the Reactor Analysis Research Group at the North-West University. This code wrapper is being developed for code coupling, uncertainty propagation, sensitivity analysis, and the development of base models. (Naicker, 2021)

NWURCS can be used to generate input files for KENO-VI, NEWT and MCNP6. NWURCS uses the level scheme structure. The starting cell is identified and then the unit to lattice method is followed. The unit and lattices are nested within each other in order to follow the level structure (Naicker, et al., 2021). For example, unit00002 may contain 7 volumes (cells), each volume will specify whether it contains a specific lattice (example lattice00001). Lattice00001 will then specify the units it is filled with. This combination continues until level 3, which in the context of the spent fuel pool will be the fuel pin. In this study, the level structure was applied as illustrated in Figure 4-3.

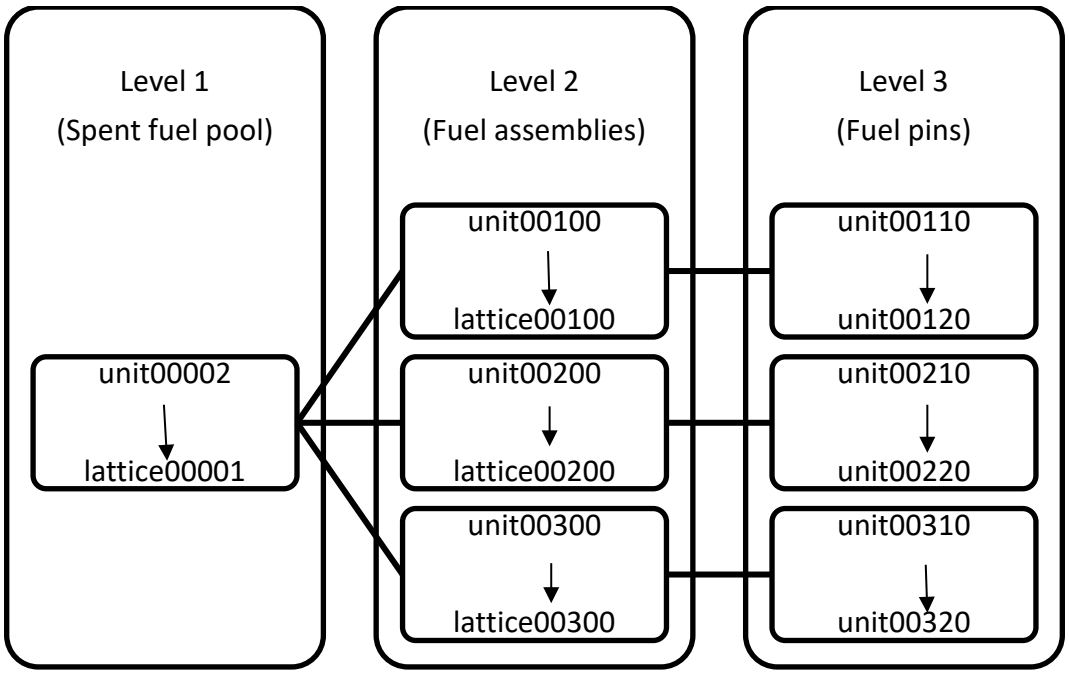

Figure 4-3: NWURCS nested structure

4.6 MCNP6

4.6.1 MCNP6 input file

The MCNP6 code input file has three main sections namely: cell data, surface cards and data cards. The input file gives a description of the problem geometry, material and source specification and defines the calculation results that are required. The input follows a fixed structure as shown below.

Title Card
Cell Cards
Blank Line Delimiter
Surface Cards
Blank Line Delimiter
Data Cards
Blank Line Delimiter

Title card
The title card is determined by the user to name or define the model to a title that is user-friendly.

Geometry: surface and cells

MCNP6 geometry is defined by 3-D configurations of user defined materials in geometrical cells bound by first- and second-degree surfaces. Cells are defined by intersections, unions and complements of regions bounded by surfaces. The surfaces are defined by providing coefficients to the analytical surface equations.

The surface card is written as follows:

J (n) a (list)

where *j* is the cell identifier surface number, n is used for coordinate transformation, a is an equation mnemonic and "list" are the parameters of the equation mnemonic.

Example

2 px -137.586670

Note that in the above example, the coordinate transformation is not shown.

Cells

Cells are used to define objects in MCNP6. Cells use the form.

J m d geom (params)

Where *j* in the cell number and *m* is the material number which must correspond with the number specified in the Mm card. Zero (0) is used to indicate that a cell is void. *d* is the material density noting that when the material number is positive, then MCNP6 interprets this as atomic density in units of 10^3 atoms/cm^3 and when it is negative then MCNP6 interprets this as mass density in units of g/cm^3. *Geom* specifies the geometry of the cell where *Params* is for cell parameters specifications defining the geometry. This can consist of a list of surfaces. In the example given next, one surface is used to define the cell. (Boston, 2014).

An example of an MCNP6 cell is

100107 7 0.0876577 -52

MCNP6 uses the methods of absorption, collision, and track length to calculate the k_{eff}or k_{inf} for each neutron history in the cycle. *kcode* is required by MCNP6 to run a criticality calculation. The code then uses a combination of different methods to provide a combined k_{eff} or k_{inf} estimate (Goorley, Tim; Los Alamos National Laboratory,X-5, n.d.). In MCNP6, the format of *kcode* is as follows:

kcode *nsrck* *rkk* *ikz* *kct*

Where:

kcode is the card name for criticality,

nsrck is the number of source neutrons per cycle,

rkk is the initial guess for k_{eff},

ikz is the number of cycles skipped before accumulating data, and

kct is the total number of cycles to be run.

Example of the *kcode* command

kcode *100000* *1.50000* *150* *250*

4.7 KENO-VI models

KENO-VI is a multigroup Monte Carlo code for evaluating k_{eff} or k_{inf} in 3-D systems. The model can be described using basic geometry bodies such as cuboids, cones, circles, and arrays. In KENOV.a, 2-D colour plots of the geometry model can be generated, or the model can be displayed in 3-D using the KENO-3D visualization tool. (Busch & Bowman, 2003). KENO-VI models were generated using NWURCS. The NWURCS code generates a KENO-VI input file parallel to MCNP6. The input file was then run as "runk" on the command prompt screen.

4.8 Boundary conditions

In this study we focused on void boundary conditions and periodic boundary conditions. Void boundary conditions take into consideration the finite size of the spent fuel pool. Periodic and reflective boundary conditions are a collection of boundary conditions used to approximate a vast (infinite) system using an appropriate combination of unit cells. Another way of describing this is that there is no neutron leakage from the system. The spent fuel pool as shown in Figure 3-4 consists of a number of arrays. In modelling a single array, for example the array in region 2, B2, it can be seen that there are neighbouring arrays on the left, right, and top, but not at the bottom. A periodic boundary condition on the top allows the top neighbour to be accounted for to a certain extent, but this then means that the bottom side would also have a lattice neighbour, which is not correct. However, modelling the bottom as void, will then mean that the top should also be modelled as void, and the top lattice neighbour would not be considered. A full spent fuel pool calculation where all the arrays are modelled would not have this problem, as all sides can have a void boundary condition.

However, in this study, the periodic boundary condition was chosen so as to be consistent with the COLA model.

Therefore, the base model uses boundary conditions where x and y boundaries are periodic, whilst the z boundary is void.

At this point, it is important to distinguish between the effective multiplication factor k_{inf} and the infinite multiplication factor k_{inf}.

When a system is modelled with periodic or reflective boundary conditions, then with the system being infinite in the relevant directions, the term ‘k-infinity’or k_{inf} is used. When the system is modelled with void boundary conditions at all boundary surfaces, then the term “k-effective” or k_{inf} is used. In this work, the fuel assemblies and the spent fuel pool array have reflective and periodic boundary conditions respectively, therefore the term k_{inf} is used in all cases.

CHAPTER 5 RESULTS AND DISCUSSION

Chapter overview

This chapter shows the analysis of all the objectives described in Section 1.3. First a NEWT model was developed for the fuel assembly to facilitate the burnup calculations of the fuel assembly so that the isotopic concentration of the spent fuel assembly can be obtained to be used in the SFP calculation. The NEWT discussion includes k_{inf} convergence, isotopic characterization and burn-up.

These are then followed by the spent fuel pool modelling.

NWURCS is also used to generate MCNP6 and KENO-VI models for the spent fuel pool according to one of the models defined in the COLA document. This model specifications are provided in annexure 2.

The boron test and other sensitivity studies were carried out to verify this model.

5.1 k_{inf} convergence

The results discussed in this section show the convergence of the local grids for the fuel assembly. The method used to obtain these results is described in Section 4.3. The convergence of the local grids was studied by changing the number of grids in each calculation.

Table 5-1: Results for Local Grid Convergence Calculations.

Run	Global unit	Local unit	k_{inf}	$k_{inf}^{i} - k_{inf}^{40}$	Time (s)	Time (hrs)
1	64	4	1.214755	7.360E-04	2438.8	0.7
2	64	8	1.214081	6.200E-05	3417.11	0.9
3	64	12	1.213813	-2.060E-04	7757.95	2.2
4	64	16	1.213927	-9.200E-05	83229.6	23.1
5	64	20	1.213888	-1.310E-04	13800.7	3.8
6	64	24	1.213904	-1.150E-04	20341.3	5.7
7	64	28	1.213966	-5.300E-05	3244.7	9.0
8	64	32	1.214023	4.000E-06	71952.0	20.0
9	64	36	1.213986	-3.300E-05	85970.0	23.9

10	64	40	1.214019	0	169795.0	47.2

The data shows that the convergence of the local grid is within 20 pcm which can be observed in Figure 5-1. (The unit pcm is calculated by multiplying the difference of reactivities by the factor 10^5. When k_{inf} is close to 1.0, then the differences in k_{inf} can be approximately given in units of pcm as well). The smaller the grid size (more grids), the more time needed to complete a calculation. The data starts to converge at approximately 28 local grids. From this, we observe that the values of k_{inf} converge as the number of grids increase.

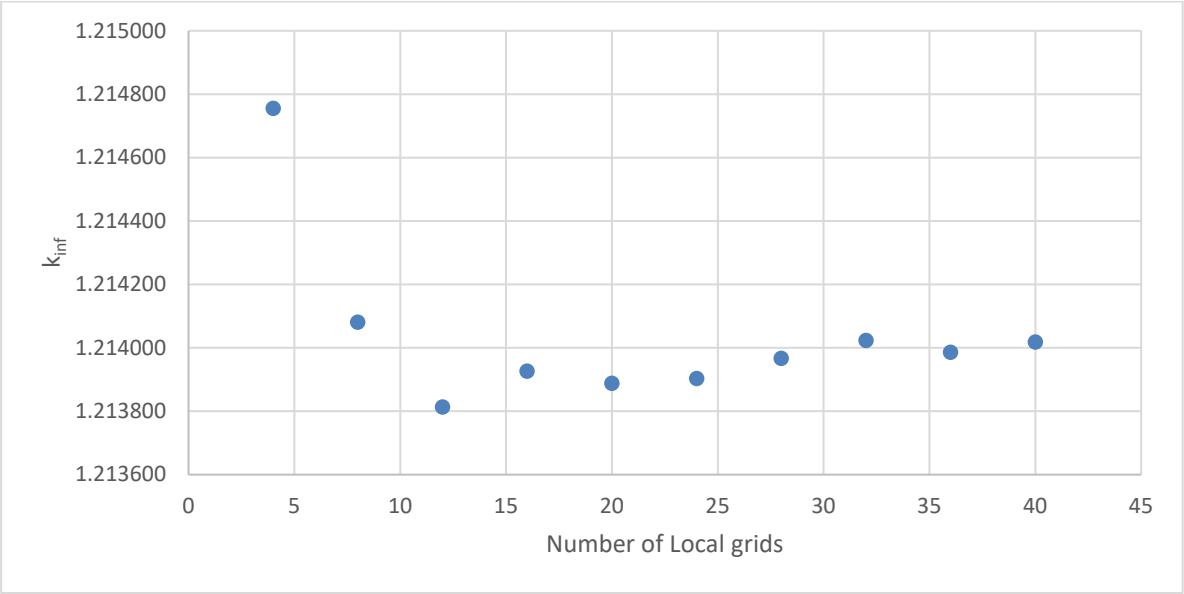

Figure 5-1: k-inf vs Number of local grids

The same trend can be observed from Figure 5-2 below for the local grids.

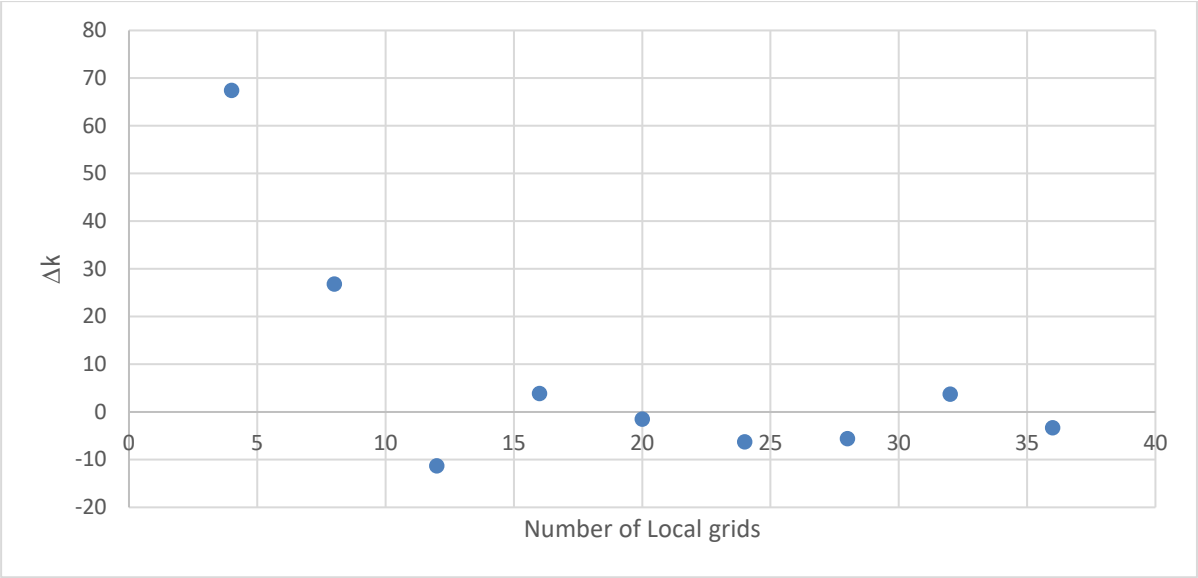

Figure 5-2: Δk vs local grids

For all the other models in this study, it has been concluded that the grids where k_{inf} converges will be used for calculation, based on the figures above.

5.2 Burn-up model comparison

The spent fuel pool base model consists of a fresh fuel assembly with enrichment of 1.6wt% and 5wt% shown in Section 4.2. 1.6wt% was used to approximate the spent fuel assembly. In reality, there is no fresh fuel assembly with an enrichment of 1.6wt%. However, as explained earlier, at the end of three cycles of burnup in the reactor core, the enrichment of the fuel for the given reactor scenario will be close to 1.6wt%. Furthermore, the spent fuel assembly will also have different concentrations for the U-238 and other isotopes of uranium and there will be transuranic products such as plutonium, together with xenon, and other fission products.

In order to get an indication of how significant this is, the fuel assembly with 3.1wt% was burnt for 4.5 years such that the end enrichment was close to that of 1.6wt%. In order to achieve this, the power was adjusted appropriately. Table 5-2 below shows the power profile adjustments, linear interpolation was made in order to obtain a close approximation of the power.

It is noted that the 5wt% enrichment of the fresh FA loaded into the SFP represents the upper limit of the possible FA that can be stored in the SFP before use in the reactor. However, 3.1wt% enrichment was used as the starting enrichment for the burnup calculation, since this represents the likely FAs that were loaded into the reactor core.

Table 5-2: Power profile study

Case	Power (MW/MTHM)	Number densities (atoms/barn.cm)	
		Start of burn-up	End of burn-up
NWURCS		7.2909E-04	3.7631E-4
Burnupcalc_3.1%FA_1	17.67546	7.2909E-04	2.1754E-04
Burnupcalc_3.1%FA_2	27.67546	7.2909E-04	9.3863E-05
Burnupcalc_3.1%FA_3	7.67546	7.2909E-04	4.4512E-04
Burnupcalc_3.1%FA_4	37.67546	7.2909E-04	3.6240E-05
Burnupcalc_3.1%FA_5	40.67546	7.2909E-04	2.6844E-05
Burnupcalc_3.1%FA_6	47.67546	7.2909E-04	1.3136E-05
Burnupcalc_3.1%FA_7	38.67546	7.2909E-04	3.2809E-05
Burnupcalc_3.1%FA_8	39.67546	7.2909E-04	2.9685E-05
Burnupcalc_3.1%FA_9	10.71511	7.2909E-04	3.6228E-04
Burnupcalc_3.1%FA_10	10.2024	7.2909E-04	3.7534E-04

The OPUS model uses the OPUS block in SCALE to specify the burn-up isotopes to be studied in the spent fuel pool, while the default isotopes are generated by the code when the OPUS block is not defined.

Figure 5-3 shows the list of the important nuclides that have been used in the opus block. Based on Table 4-2, these nuclides were then burnt (produced in the burnup calculation) and then utilized as inputs to spent fuel pool model.

```
read opus
  units=atom
  volume=1
  symnuc=
    u-234   u-235   u-236   u-238   pu-238  pu-239  pu-240
    pu-241  pu-242  pu-243  ag-107  ag-109  am-241  am-242
    am-243  cd-106  cd-108  cd-110  cd-111  cd-112  cd-113
    cd-114  cd-116  cm-242  cm-243  cm-244  cm-245  cs-133
    cs-134  cs-135  cs-137  eu-153  eu-154  eu-155  gd-154
    gd-155  in-113  in-115  mo-95   np-237  nd-143  nd-144
    nd-145  nd-146  nd-148  nd-150  np-237  o-16    pb-206
    pb-207  pb-208  pd-105  pm-147  pr-141  rh-103  ru-101
    sm-147  sm-148  sm-149  sm-150  sm-151  sm-152  sm-154
    tc-99   xe-131
            end
  matl=0 1  end
end opus
```

Figure 5-3: List of important nuclides based on SCALE

The results of the spent fuel pool criticality calculation with these isotopes can be seen in Table 5-3 below. It was observed that MCNP6 and KENO-VI results are in very good agreement and have a delta of 72 pcm, which is less than three times the standard deviation of each calculation. This delta in units of pcm is calculated as MCNP6 k_{inf} subtracted from KENO-VI k_{inf} multiplied by a one hundred thousand.

Table 5-3: Burnt SFP results

Name	**Value**
KENO-VI	1.01679
Std dv	0.00030
MCNP6	1.01751
Std dev	0.00024
Delta	-72

The results for the second calculation, in which the depleted fuel assembly only contained 1.6wt% U-235 are shown in Table 5-4. Furthermore, it was noted that there was good correspondence between the MCNP6 and KENO-VI calculations.

Table 5-4: burnt SFP for 5wt% and 1.6wt%

Name	**Value**
KENO-VI	0.98897
Std dev	0.00028
MCNP6	0.98965
Std dev	0.00019
Delta	-68

However, it was observed that when the burnt isotopes are included the depleted assembly specification, k_{inf} increases instead of decreasing. One would have expected, with the inclusion of the fission products, that k_{inf} would have decreased. This is because fission products are neither fissile nor fissionable, and therefore will also act as absorbers. In order to investigate this further, calculations were carried out in which isotopes were added one at a time or in groups when expected to behave in the same way.

Table 5-5: Indicates all the cases and their respective change in k_{inf} in pcm.

Case	Changes	KENO-VI k_{inf}	std dev	Pcm
1	Initial	0.98897	0.00028	0
2	Concentration of O-16	0.98868	0.00024	-29
3	Concentration of u-235 changed from 3.8620e-4 to 3.8621e-4	0.98838	0.00023	-30
4	Concentration of u-238 changed from 2.3452e-2 to 2.2240e-2	0.99361	0.00026	523
5	u-234 added	0.99316	0.00026	-45
6	u-236 added	0.99151	0.00027	-165
7	Fission products added	0.96080	0.00027	-3071
8	Am-241/243 added	0.96102	0.0003	22
9	Am242 added	0.98838	0.00032	2736
10	Cm242/244 added	0.96008	0.00024	-2830
11	Cm 243/245 added	0.96017	0.0003	9
12	Np-237 added	0.95901	0.00027	-116
13	Pu-238 added	0.95931	0.00029	30
14	Pu-239 added	1.03223	0.00025	7292
15	Pu-240 added	1.00887	0.00026	-2336
16	Pu-241 added	1.01767	0.00024	880
17	Pu-242 added	1.01751	0.00028	-16
18	Pu-243 added	1.01679	0.0003	-72

The increment changes were made to the 1.6wt% fuel assembly so that it matches the burnt fuel assembly composition Table 5-5. When the resonance absorbers were decreased in concentration, k_{inf} increased as is expected (as observed in Case 4). The concentration of U-238 should decrease with burnup since it gets transmuted when absorbing a neutron. When resonance absorbers and fission products were added the value of k_{inf}decreased, as can be seen in cases 5, 6 and 7, respectively. It was also noted that the fission products (in case 7) showed a large decrease in k_{inf} As mentioned above, this is because fission products are not fissile or fissionable, and therefore will also act as absorbers. In terms of the transuranic isotopes, the fissile isotope Pu-239 was the highest contributor shown in case 14 with an increased k_{inf}value. Pu-241 and Am-242 also contributed significantly to the increase in k_{inf}. On the other hand, Cm-242, Cm-244 and Pu-240 decreases k_{inf} significantly.

In the pcm column, the negative sign indicates the decrease in k_{inf} and the positive value indicates the increase in k_{inf}. In appraising this column, one therefore realizes that there are both positive (increasing) and negative (decreasing) of the isotopes to k_{inf}, with the large contribution from Pu-239. The reasons for these positive or negative contributions were given in the preceding paragraphs. Adding all these contribution (positive and negative) yields the net effect that the multiplication factor increases.

Furthermore, a boron study was carried out on the burnt isotopic SFP model. The amount of boron in the system was increased and the effect on the multiplication factor was observed. Table 5-6 below shows the results for this boron test. It was observed that the system will have a k_{inf} value of 0.95 below 256 ppm. Although the value for k_{inf} is greater than 1.00 in the model with fission products and transuranic isotopes, k_{inf} will reduce to the required value of 0.95 when boron is added into the system.

Table 5-6: Loaded SFP boron test

Boron concentration (ppm)	KENO-VI k_{inf}	std dev
0	1.01679	0.00030
150	0.96593	0.00024
200	0.95783	0.00030
250	0.95082	0.00025
256	0.95010	0.00028
260	0.94963	0.00026
270	0.94817	0.00031
300	0.94347	0.00029
600	0.90455	0.00024

Figure 5-4 below shows the boron results for the loaded spent fuel pool. k = 0.95 can be interpolated on the graph.

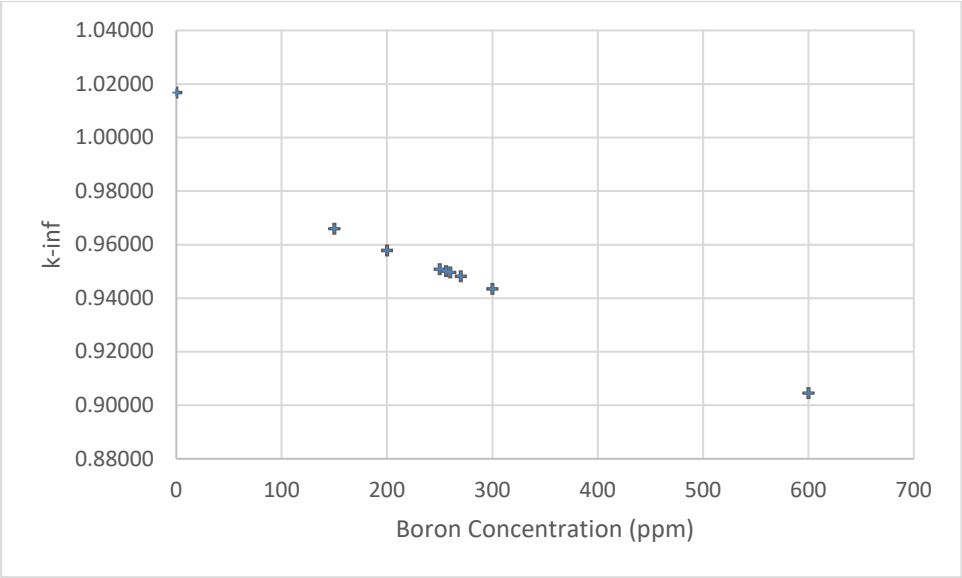

Figure 5-4: k_{inf} vs boron for loaded spent fuel pool

5.3 Model verification

This study was also used to verify NWURCS capabilities for spent fuel pool calculations. NWURCS used in this study is a beta version, which may have programming errors. It is used to generate input models for PWRs (including the EPR) and now for a spent fuel pool. Input files for several codes such as MCNP6 and KENO-VI are generated. NWURCS simplifies the process to write input files for the codes mentioned above. It is thus important to verify the code to ensure that there are no "mix up" in the way the input files are produced. The following sections discusses the various methods used to verify the model. In summary, these were visual inspection of the geometry plots, and line by line inspection of the materials as listed in the material input file.

In addition, the inspection of the input file in terms of the nested levels was also carried out, and these levels were shown to be consistently defined. This last task is not discussed below. However, it meant working though the input lines, and verifying that the volumes fitted within the lattices of the three levels and also that the materials were defined correctly.

5.3.1 Spent fuel pool

The spent fuel pool consists of separate regions as discussed in Section 3.2.1. Figure 5-5 below verifies that the structure of the region modelled in this study is correct and shows the layout of the spent fuel pool region. One can see that the structure is 12 x 12 in counting the blocks. Additionally, the detail that each block contains a fuel assembly can be seen, thus showing the nested nature of the modelling.

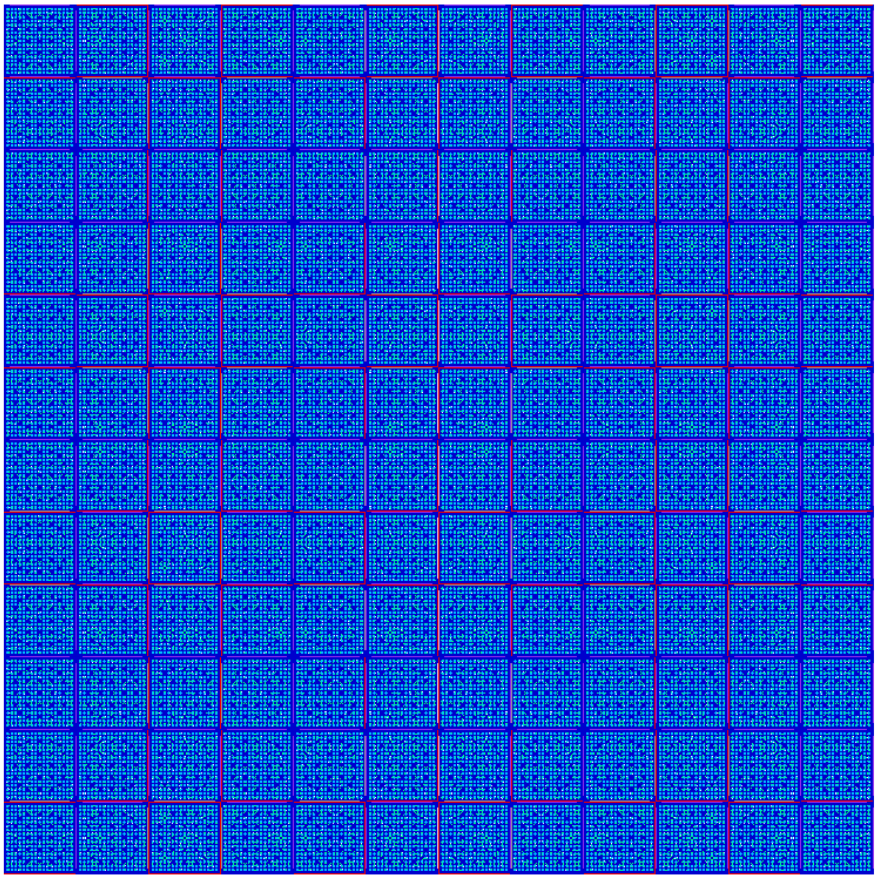

Figure 5-5: Spent fuel pool region 2 layout

Figure 3-5, Figure 3-7 and Figure 3-8 shown in Chapter Four also verify the layout of this region. In Figure 3.5, the axial view is shown. One can see the various structures, starting from the bottom, and moving to the top. These included the base plate (volume 6), the pedestal (volume 5) and the spent fuel assemblies (volume 3).

In Figure 3-6 the 12 x 12 spent fuel pool array is shown. One can count the 144 fuel assemblies, and also note the 17 by 17 arrays in each fuel assembly, although not clearly. However, the distinct

layout of the guide tubes in each fuel assembly can be observed. The detail of the metamic structure cannot be seen, and therefore this detail is shown in Figure 3-7.

In Figure 3-7, the details of a section of the spent fuel assembly are shown. The metamic plates and the stainless-steel plates are shown to have the correct geometry, thus verifying this part of the model.

5.3.2 Material verification

The material specifying file, inputmat, was visually inspected to verify the materials, material numbers, densities and their correct usage in the lattice and unit files. This can also be verified by the output files.

The inputmat file describes the materials used in the development of the geometry. Below is a sample of the structure of the inputmat file. In the Figure 5-6, water and helium can be seen, and other details required by NWURCS.

```
1  water___
2  none
3     1    1
4     1    1
5     1.000      100     2
6       1   2.0   0
7       8   1.0   0
8  He______
9  none
10     2    1             material no
11     0                  MCNP     s(a,b)
12   0.0015981   100    1 Density, % binary mixture(u3+ s2),2 entries follow
13     2   1.000000   0    He
```

Figure 5-6: NWURCS material input

Figure 5-7 below shows a section of the spent fuel racks that have been developed, the different materials and how the Metamic panels, void gap and sheathing panels fit together on the storage cell and how they continue into the developed cell. This figure is similar to Figure 3-8 in Chapter three, however in this section it is shown to verify that the materials are assigned correctly. This is a visual verification, with the material shown as pink, purple and red being the Metamic, void and stainless steel respectively. The development of the racks was successful based on the description given in the COLA system. FULCRUM and the input file for KENO-VI were used to get the visual representation of the system.

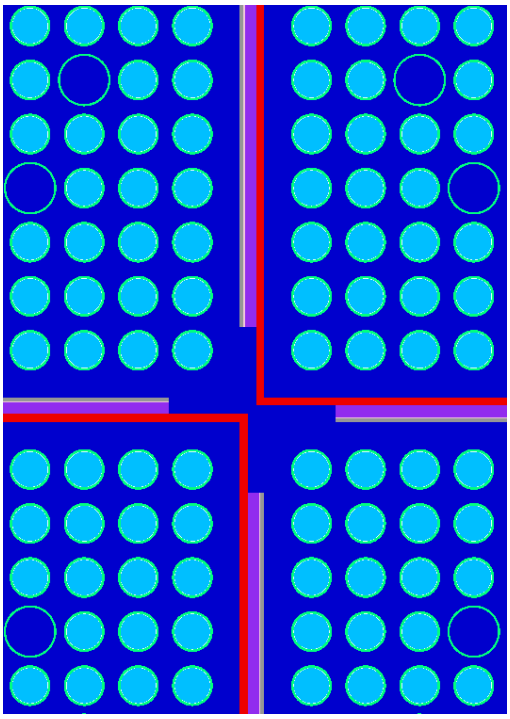

Figure 5-7: Cross section of spent fuel pool

5.3.3 Volume verification

All the volumes from volume 1 to volume 7 are axially stacked on top of each other to form a "tower" like structure. These volumes are discussed in Section 3.2.1 and are shown in Figure 5-8 and Figure 3-5

Volume 1 to 7 are cuboids. Looking at the XY dimensions of the system all the volume dimensions are the same. This was done by visually inspecting the input file and manually calculating the dimensions to see whether they correspond with those generated by NWURCS.

To show the level structure discussed in Section 4.5 we consider volume 3 which is filled with lattice00002. The lattice is a 12 x 12 lattice and fits into volume 3. Each unit has a lattice parameter of x=13.84300 x 2 and y=13.84300 x 2. The structure that fits into volume 3 has a size of 332.323 cm in both the x and y directions. This means x_1 = -166.116 cm, x_2 = 166.116 cm, y_1 = -166.116 cm and y_2 =166.116 cm when the centre of the unit is set to be 0.0 cm.

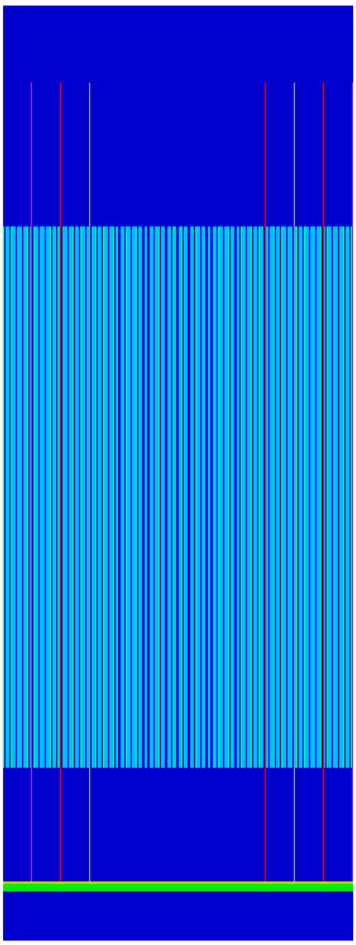

Figure 5-8: Spent fuel pool side view

5.4 Model analysis

One of the objectives of this study was to build a MCNP6/KENO-VI model of the spent fuel pool. As was mentioned, NWURCS is being developed by the research team to build such a model, together with other models for other nuclear systems not applicable to this study. The level structure employed in NWURCS leads to a general model structure. Therefore, each reactor system that can be modelled using NWURCS must be verified individually. The one choice for verification was to verify a NWURCS model based on a model available in the open literature, with published results. As discussed in Section 4.4, this was the model listed in Table 2.11 of the COLA specification. This model was chosen because of its simplicity. Region 2 of the SFP was modelled, only one fuel assembly was modelled of enrichment 2.07wt% U-235, and only one temperature was specified for all the materials. In Table 5-7 the results of the base model is shown. The COLA system gives a k_{inf} nominal value of 0.97064, whereas the base model calculation in this study gives a k_{inf} value of 0.97421. These values have a difference of -357 pcm.

Table 5-7: Illustrate the Base Model Results

	KENO-VI		**MCNP6**		**1 SIGMA**	
	k_{inf}	std dev	k_{inf}	std dev	MIN	MAX
Base model	0.97421	0.00026	0.97525	0.00020	0.97395	0.97447
COLA	0.97064	0.00051	-	-	0.97013	0.97115
PCM	-357	25	-	-	-382	-332

The pcm value was reduced during the boron test, as discussed in the next section 5.4.1, giving agreeable results. Another possible contribution to the difference in the k_{inf} is in terms of the code and nuclear data library used.

The COLA system uses the SCALE-4.4a version with the evaluated nuclear data file version given in 44-groups. This is version 5 of the neutron cross section library (ENDF/B-V).

However, this study used SCALE-6.2.3 with nuclear data file ENDF/B-VII. The generation of MCNP6 input files for the spent fuel pool using NWURCS is discussed in the Chapter 4. KENO-VI and MCNP6 use ce-v7 and TRITON uses v7-252.

5.4.1 Boron test

The COLA document makes no mention of the exact amount of boron present in the spent fuel pool. However, it indicates that a boron of 948 ppm yields a k_{inf} of 0.95. A boron test was carried out where the concentration of boron is varied in order to obtain a k_{inf} within the statistical error of the COLA k_{inf}. As given earlier, k_{inf} of 0.97421 is obtained when the system has no concentration of boron. This is off by 357 pcm from the k_{inf} value given in Table 2-11 for the COLA system in the COLA document. Table 5-8 below gives the results obtained. The delta values are calculated as the k_{inf} difference between KENO-VI and MCNP6 multiplied by $1x10^5$

Table 5-8: k_{inf} results for varied Boron concentrations for a 12 by 12 system

Boron concentration(ppm)	KENO-VI		MCNP6		Delta
	k_{inf}	std dev	k_{inf}	std dev	
1000	0.94358	0.00034	0.94378	0.0002	-20
800	0.94925	0.00027	0.95028	0.00021	-103
600	0.95505	0.00028	0.95596	0.00023	-91
400	0.96180	0.00024	0.96246	0.00021	-66
200	0.96809	0.00026	0.9686	0.0002	-51
175	0.96885	0.00023	0.96966	0.00021	-81
150	0.96969	0.00028	0.97015	0.0002	-46
125	0.97011	0.00028	0.97121	0.0002	-110
115	0.97048	0.00024	0.97137	0.00022	-89
110	0.97116	0.00026	0.97158	0.0002	-42
100	0.97168	0.00022	0.97188	0.00019	-20
50	0.97284	0.00028	0.97316	0.0024	-32
0	0.97421	0.00026	0.97525	0.0002	-104

The COLA k_{inf} of 0.97064 has a standard deviation of ± 0.00051. In terms of a minimum and maximum limits, intervals of (0.97013, 0.97115) for one sigma and (0.96911, 0.97217) for three sigma were obtained, respectively. For a k_{inf} within three sigma standard deviation the nominal value for the COLA results of Table 2-11 in the document is obtained when the boron concentration is 125 ppm and within 1 sigma at a boron concentration of 115ppm.

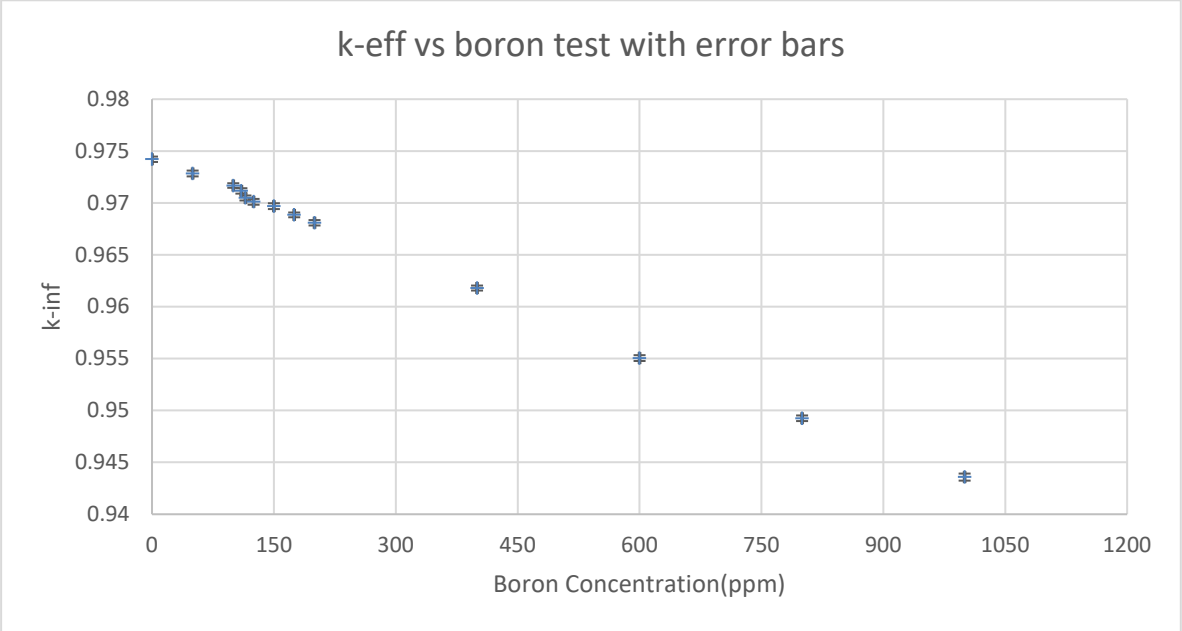

Figure 5-9: Boron test results

Figure 5-9 above shows that the k_{inf} value decreases as the concentration of boron increases, which was expected. The results can be used to interpolate the corresponding boron value for k = 0.95. This value of k_{inf} is calculated by interpolation when the boron concentration is approximately 668.5ppm. The relationship between boron and the k_{inf} value can be explained using the one group reactor equation as discussed in Section 2.7. Figure 5-10 shows the k_{inf} against the boron concentration for results obtained using KENO-VI and MCNP6. It can be observed that the results given by the two codes are similar. Figure 5-10 shows the comparison between the k_{inf} obtained in KENO-VI and the k_{inf} obtained in MCNP6. It can be observed that the k_{inf} on both codes follow a similar pattern.

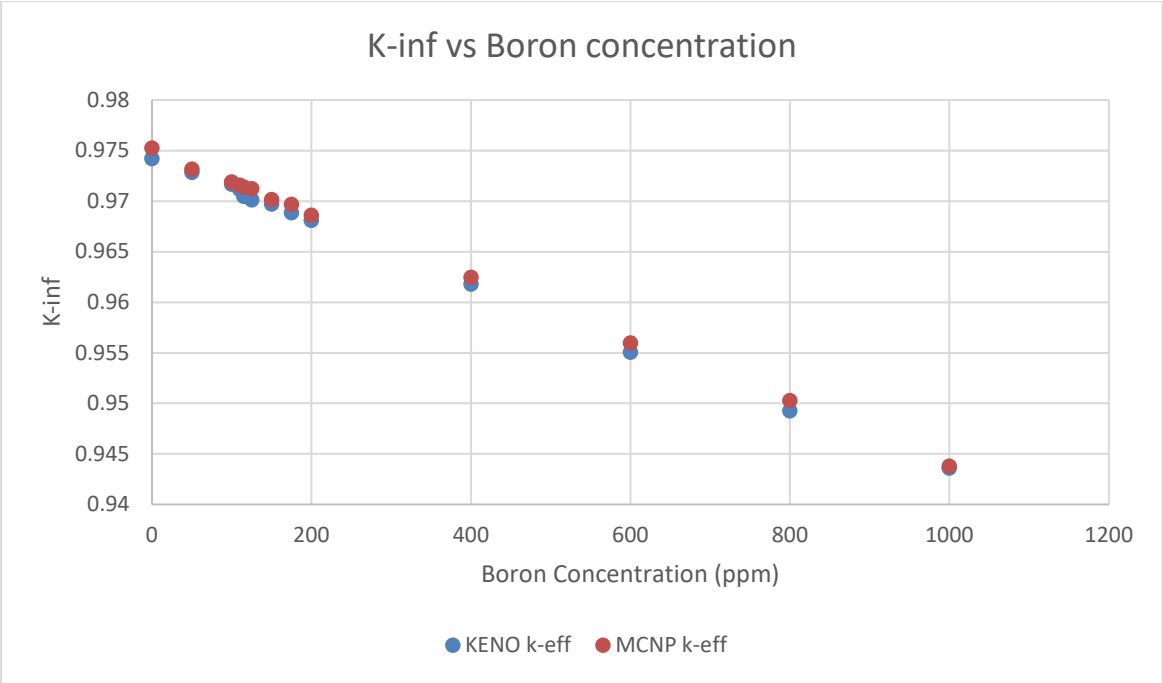

Figure 5-10: k_{inf} vs boron concentration

Table 5-9 below shows the difference between the COLA nominal value (in pcm) for k_{inf} and k_{inf} for the boron tests performed.

The boron tests carried out in this study agree with these values as it can be observed that at 120 ppm, the k_{inf} value agrees with that reported in the COLA document. The value of 120 ppm is taken as the average of 125 ppm and 115 ppm reported in the first paragraph of this section. These results therefore provide confidence in the model that was developed in this study. The difference between the k_{inf} nominal COLA value and the k_{inf} values obtained in this study is also given Table 3-1 for numerical record. This records which boron concentration yields a k_{inf} closest to that of the COLA document.

Table 5-9: pcm table for COLA vs modelled KENO-VI results

Boron concentration	k_{inf}	std dev	pcm (Cola k_{inf} vs KENO-VI)
COLA	0.97064	0.00051	0
1000	0.94358	0.00034	2706
800	0.94925	0.00027	2139
600	0.95505	0.00028	1559
400	0.9618	0.00024	884
200	0.96809	0.00026	255
175	0.96885	0.00023	179
150	0.96969	0.00028	95
125	0.97011	0.00028	53
115	0.97048	0.00024	16
110	0.97116	0.00026	-52
100	0.97168	0.00022	-104
50	0.97284	0.00028	-220
0	0.97421	0.00026	-357

5.4.2 Spent fuel pool sensitivity analysis

This section shows the sensitivity results based on the COLA sensitivity study. The COLA sensitivity study was based on Table 2-11 of the COLA document. Both KENO-VI and MCNP6 models were used. Different parameters were used, and the sensitivity study was carried out to study the effects of each parameter. The parameters studied are shown in the Table 5-10 below. The analysis looked at k_{inf} and the standard deviation in KENO-VI and MCNP6. There is good agreement between these two sets of results. Increasing the enrichment caused the k_{inf} to increase, as predicted by the one group equation. The increase in the fuel pellet outer diameter also increased the k_{inf}. When reducing the cladding outer diameter, the k_{inf} increases, since by reducing the cladding diameter, the moderator volume (water) is increased, which leads to more moderation of the neutrons.

The North Anna density was included in the sensitivity studies in order to study the model in a scenario of using the North Anna density instead of the COLA density.
The boundary conditions sensitivity was also included in the study and for the reflected boundary conditions, the value of k_{inf} increases since there is no neutron leakage.

Table 5-10: Spent fuel pool sensitivity analysis

Sensitivity			KENO-VI		MCNP6		KENO-VI – MCNP
	Initial value	**change**	k_{inf}	**std dev**	k_{inf}	**std dev**	
Nominal value	-	-	0.97421	0.00026	0.97525	0.00020	-0.00104
Fuel enrichment(+0.05wt)	2.07	2.12	0.98204	0.00027	0.98207	0.00020	-0.00003
Density (+1%)	10.686	10.736	0.97490	0.00023	0.97599	0.00024	-0.00109
Pellet OD (+0.00127)	0.409575	0.41021	0.97508	0.00023	0.97583	0.00020	-0.00075
Clad OD (-0.00381)	0.474980	0.473075	0.97543	0.00022	0.97613	0.00020	-0.0007
North Anna fuel density	10.686	10.412	0.97074	0.00027	0.97175	0.00022	-0.00101
Boundary conditions (x&y periodic, z refl)	(x&y periodic, z void)	(x&y periodic, z refl)	0.97421	0.00026	0.97500	0.00021	-0.00079
Boundary conditions	(x&y periodic, z void)	Void	0.96451	0.00024	0.96517	0.00020	0.00066

The results as presented in the COLA document is shown in Table 5-11. Also shown in the sixth column is the difference between the nominal value for k_{inf} and the value for each parameter tested in units of pcm.

Table 5-11: Spent fuel pool sensitivity analysis of COLA sensitivity (Westinghouse Electric Company, 2006)

Sensitivity			COLA (Table2-11)		Delta from nominal value
	Initial value	Change	k_{inf}	Std dev	
Nominal value (COLA 2-11)			0.97064	0.00051	0
Fuel enrichment (+0.05wt)	2.07	2.12	0.97840	0.00053	-776
Density (+1%)	10.686	10.736	0.97216	0.00048	-152
Pellet OD (+0.00127)	0.409575	0.41021	0.97239	0.00049	-175
Clad od (unit710)	0.474980	0.473075	0.97266	0.00048	-202

Table 5-12 shows the sensitivity calculations of the KENO-VI model used in this study. The deviations from the nominal value are also provided in the sixth column in units of pcm.

Table 5-12: Spent fuel pool sensitivity analysis of this study

Sensitivity			KENO-VI		Delta from nominal value
	Initial value	Change	k_{inf}	std dev	
Nominal value (COLA 2-11)	-	-	0.97421	0.00026	0
Fuel enrichment(+0.05wt)	2.07	2.12	0.98204	0.00027	-783
Density (+1%)	10.686	10.736	0.97490	0.00023	-69
Pellet OD (+0.00127)	0.409575	0.41021	0.97508	0.00023	-87
Clad OD (-0.00381)	0.474980	0.473075	0.97543	0.00022	-122

Comparisons between the results in the reference COLA study and from KENO-VI of this study are shown in Table 5-13. It can be seen in this table, that the fuel enrichment difference lies within one standard deviation and this can be considered to be a good result. However, when considering differences less than three standard deviations as acceptable, then the other results can also be considered good. This verification therefore gives further confidence in the modelling approach used in this study.

Table 5-13: Delta comparison of COLA and KENO-VI

	KENO-VI difference from nominal value	Std dev	COLA	Std dev	Delta (COLA-KENO-VI)
Nominal value (COLA 2-11)	0	26	0	51	0
Fuel enrichment(+0.05wt)	-783	27	-776	53	7
Density (+1%)	-69	23	-152	48	83
Pellet OD (+0.00127)	-87	23	-175	49	88
Clad OD (-0.00381)	-122	22	-202	48	90

CHAPTER 6 CONCLUSIONS AND RECOMMENDATIONS

6.1 Conclusions

The burn-up calculations carried out on the fuel assemblies yield isotopic number densities that can be used in the criticality calculation for the spent fuel pool. These isotopes indicate the differences and changes in isotopic concentration after the initial fuel assemblies were burnt.

One of the objectives of this study was to develop a methodology that focuses on the criticality calculation of the spent fuel pool. One region of the spent fuel pool was modelled. The geometry for the base model of this region was obtained from the open-source literature. Three variations were built. In the first model, fuel assemblies of two different isotopic inventory were used. The first assembly was modelled with fresh fuel of 5.0 wt%, and the second was also modelled with fresh fuel, but with fuel enrichment of 1.6 wt% to correspond to the enrichment of the fuel (i.e., depleted fuel) when removed from the reactor core.

The first and the second models were similar in that the fresh fuel had an enrichment of 5%.
Both models also contain depleted fuel assemblies. however, In the first model, the depleted fuel assembly contained only U235 and U236 with an U235 enrichment of 1.6%. The fuel was UO_2.
In the second model, the depleted fuel assembly also contained U235 with an enrichment of 1.6%. But the U238 was lower, and the fission products and other transuranic isotopes were included. This inventory was obtained from the NEWT BU calculations.
The third model was obtained from the COLA report. This report contained a model in which fresh fuel assemblies of a single enrichment of 2.07wt% were used.
This model was therefore considered to be a good model to use to verify the models that were developed in the current work since no burnup was required.

The model with the burnt isotopes (second model) initially produced a high k_{inf}, however after performing a boron test the value for k_{inf} reduced. With the isotopes introduced into the model in a systematic way, it was found that the fissile plutonium isotopes in the model caused the increase in k_{inf}. The results served to verify the capabilities of NWURCS to perform criticality spent fuel studies.

Boron tests were performed on both the models and it was found that the boron reduces the k_{inf} value in the models. The models behaved as expected with the presence of boron in the system. The boron test performed shows that this version of NWURCS may be used to look at other variables of the spent fuel pool.

Sensitivity studies were performed as per Table 2-11 found in the COLA document. When the fuel enrichment or the density was increased, the value for k_{inf} increased. When the pellet outer diameter was increased and the cladding outer diameter was reduced, the values for k_{inf} obtained had a difference of 87 pcm and 122 pcm respectively. The changes performed for the sensitivity studies agreed with those in COLA Table 2-11.

Given the results obtained with the various tests performed, this study can then be used as a basis to perform other spent fuel pool studies, including looking at the other regions of the spent fuel and materials.
It is noted however, that the only criterion based on safety that was considered was to assess whether the multiplication factor was at 0.95 or below. Other safely factors were not considered. This was primarily due to two reasons. Firstly, the axial power profile for burnup was considered constant, and this is not the case for the actual fuel assemblies as they are burnt in the core. Secondly a constant temperature was assumed in the spent fuel pool for the fuel assemblies. Such an analysis would require thermal hydraulic considerations and will be included in future studies. Nonetheless, examining the behaviour in terms of the multiplication factor has given valuable insight into the problem.

6.2 Recommendations

6.2.1 Further Studies

- Given the applicability of this work, more studies need to be carried out to align the data used in this study with that of the spent fuel pools at the Koeberg Nuclear Power Station in South Africa.
- Studies on region one and the damaged fuel assemblies must be carried out in order to complete the regions that make up the entire spent fuel pool.
- The complete spent fuel pool must be modelled, to include region I and II

6.2.2 NWURCS

- In preparation of the input material, the fraction of the element is required. Using the natural abundance table NWURCS then calculates the number density of each isotope of the element as given by the natural abundance table. This is valid for fresh fuel and non-depleted materials. However, for depleted materials, the isotopic fractions of a given element will not be necessarily equal to the natural abundance ratios. NWURCS should therefore have this feature so that the number density of a material can have more than one definition, to account for fresh fuel and depleted fuel.

BIBLIOGRAPHY

World Nuclear Association, 2020. *World Nuclear Association.* [Online]
Available at: https://www.world-Nuclear.org/information-library/current-and-future-generation/nuclear-power-in-the-world-today.aspx
[Accessed 1 February 2020].

Boston, A., 2014. *Introduction to MCNP- the monte carlo transport code,* s.l.: s.n.

Bredell, P. J. & Stott, A. K., n.d. *Spent fuel Management in South Africa.* s.l., s.n.

Brown, F. B., 2006. *On the Use of Shannon Entropy of Fission Distribution for Assessing Convergence of Monte Carlo Criticality Calculations,* s.l.: s.n.

Busch, R. D. & Bowman, S. M., 2003. *KENO V.a Primer: A Primer for criticality calcultions with SCALE/KENO V.a Using CSPAN for input,* Tennessee: s.n.

Cetnar, J., 2006. *General solution of Bateman equations for nuclear transmutations,* s.l.: s.n.

de la Rosa Blul, J. C., McMinn, P. & Grah, A., 2018. *Analysis of the inherent response of nuclear spent fuel pools,* s.l.: s.n.

Department of Minerals Resource and Energy, 2020. *Request for information: Nuclear new build power programme,* s.l.: s.n.

DMRE, 2019. *Integrated Resource Plan.* s.l., s.n.

Dominion Nuclear Connecticut, Inc , 2012. *Criticality Safety Analysis Report (Non-Proprietary): Spent Fuel Pool Criticality.* s.l., Dominion Resources Services, Inc..

G.P. Nyalunga, V. N. K. I., 2019. Quantification and propagation of neutronics uncertainties of the Kozloduy-6 VVER-1000 fuel assembly using SCALE 6.2.1 within the NEA/OECD benchmark for uncertainty analysis in modelling of LWRs. *Elsevier,* p. 18.

Ganguly, C., 2001. Ceramic nuclear fuels for power reactors. *Proceedings - Indian National Science Academy Part A, Physical Sciences, 67(4-5), 531-574.,* pp. 531-574.

Gauld, I. C., Ilas, G. & Radulescu, G., 2011. *Uncertainties in Predicted Isotopic Compositions for High Burnup PWR Spent Nuclear Fuel,* s.l.: Oak Ridge National Laboratory.

Goorley, Tim; Los Alamos National Laboratory,X-5, n.d. *Criticality calculation with MCNP5: A primer 2nd edition,* s.l.: s.n.

Hummel , D. & Novog, D., 2011. *Joint ICTP-IAEA Course on Science and Technology of Supercritical water cooled Reactor,* Ontario: s.n.

IAEA, 2003. *STORAGE OF SPENT FUEL FROM POWER REACTORS.* Vienna, IAEA.

IAEA, n.d. *International Atomic Energy Agency.* [Online]
Available at: https://www.iaea.org/topics/response/fukushima-daiichi-nuclear-accident
[Accessed 11 11 2021].

Kim, K.-S. & DeHart, M. D., 2010. *Unstructured partial- and net-current based coarse mesh finite difference acceleration applied to the Extended Step Characterization method in NEWT,* s.l.: s.n.

Lamarsh, J. R. & Baratta, A. J., 2001. *Introduction to Nuclear Engineering.* 3rd ed. New Jersey: Prentice Hall.

Los Alamos National Laboratory, 2017. *Monte Carlo N-Particle Transport Code System Version 6.2,* New Mexico: Radiation Safety Information Computational Center(RSICC).

Metals, A., 2015. *ATIMetals.* [Online]
Available at:
https://www.atimetals.com/Products/Documents/datasheets/zirconium/alloy/Zr_nuke_waste_disposal_v1.pdf
[Accessed 26 June 2020].

Montwedi, O. E., 2014. *Neutronic simulation of a European Pressurised Reactor,* s.l.: s.n.

Naicker, V., 2021. *NWURCS USER MANUAL VERSION 3.1,* s.l.: s.n.

Naicker, V. V., Sihlangu, S. F., Hou, J. & Reitsma, F., 2021. *Uncertainty Propagation for the HTTR in terms of the IAEA CRP on HTGR Uncertainty Analysis in Modelling.* Yogyakarta, Indonesia, s.n.

National Nuclear Regulator, 2017. *South African national report on the compliance to obligations under the joint convention on safety of spent fuel management and on the safety of radioactive waste management,* s.l.: s.n.

NEI & Dominion, 2008. *Economic Benefits of North Anna Power station,* s.l.: s.n.

NRC, 2017. *United States Nuclear Regulatory Commission.* [Online]
Available at: https://www.nrc.gov/waste/spent-fuel-storage/pools.html
[Accessed 26 May 2020].

Nuclear Energy Agency, 2015. *Status Report on Spent Fuel Pools under Loss-of-Cooling and Loss-of-coolant Accident Conditions,* s.l.: s.n.

Nuclear Regulatory Commission, 2014. *Briefing on spent fuel pool safety and consideration of expedited transfer of spent fuel to dry casks.* s.l., NRC.

Nyalunga, G., 2019. *Quantifying uncertainties of aspects of the neutronics modelling of the Kozloduy-6 system using SCALE 6.,* s.l.: s.n.

Nyalunga, G., Naicker, V. & du Toit, M., 2016. Developing skills for neutronic modelling of nuclear power reactors in South Africa. *Journal of Energy in Southern Africa,* Volume 27.

Rearden, B. T. & Jessee, A. M., 2018. *Scale Code System,* s.l.: s.n.

Rosenfeld, P. E. & Feng, L. G., 2011. *Risks of Hazardous waste,* s.l.: s.n.

Shultis, J. K. & Faw, R. E., n.d. *An MCNP Primer,* s.l.: s.n.

Sigman, K., n.d. *Random Mumber Generators,* New York: Columbia University-Department of IEOR.

Stacey, W. M., 2007. *Nuclear Reactor Physics.* Second edition ed. s.l.:Wiley-VCH.

The Virtual Nuclear Tourist, n.d. *Nuclear Power Plants - South Africa.* [Online]
Available at: http://www.nucleartourist.com/world/koeberg.htm
[Accessed 21 03 2022].

Thokwane, K. M., 2020. *Initial implementation of the neutronics codes DRAGON and DONJON at the North-West University,* s.l.: s.n.

VEPCO, 2009. *North Anna Power station Updated Safety Analysis Report,* Virginia : s.n.

Westinghouse Electric Company, 2006. *AP1000 Standard Combined License Technical Report: Spent fuel Storage Racks Criticslity Analysis,* Pittsburgh: s.n.

World Nuclear Association, n.d. *World Nuclear Association.* [Online]
Available at: https://world-nuclear.org/information-library/country-profiles/others/emerging-nuclear-energy-countries.aspx
[Accessed 22 February 2022].

World Nuclear Association, n.d. *World Nuclear Association.* [Online]
Available at: https://world-nuclear.org/information-library/safety-and-security/safety-of-plants/safety-of-nuclear-power-reactors.aspx
[Accessed 22 February 2022].

Wu, S.-C., Chao, D.-S. & Liang, J.-H., 2018. *Influence of simultaneous variations in operating parameters on burnup,* s.l.: s.n.

ANNEXURES

ANNEXURE 1

In the following annexure, the tables for the COLA design input for region 1 and region 2 can be found. All the values are in inches and have been converted into centimetres in this study.

Table 2-5 Design Input for Region 1 Storage Racks (All dimensions are in inches; tolerances are not shown because they are Westinghouse Proprietary Information.)

Parameter	Value
Storage Cell Center-to-Center Pitch	10.9
Storage Cell Inner Dimension (Width)	8.8
Inter-Cell Flux Trap Gap	1.644
Storage Cell Length Region 1 Spent Fuel Storage Rack New Fuel Storage Rack	 199.5 193.5
Storage Cell Wall Thickness	0.075
Neutron Absorber Material	Metamic
Neutron Absorber Length	172
Neutron Absorber Width	7.5
Neutron Absorber Thickness	0.106
Distance from Top of Rack Baseplate to Bottom of Neutron Absorber	6.23
Neutron Absorber B_4C Loading	31 weight-percent
Neutron Absorber Sheathing Thickness Internal Walls Periphery Walls	 0.035 0.075
Baseplate Thickness	0.75
Baseplate Flow Hole Diameter	6
Rack Pedestal Type (fixed or adjustable)	Adjustable
Rack Pedestal Height (female + male)	2.75
Rack Female Pedestal Dimensions	20 x 20 x 2.25
Rack Male Pedestal Diameter	4.5
Rack Bearing Pad Thickness	1.5

Table 2-6 Design Input for Region 2 Storage Racks
(All dimensions are in inches; tolerances are not shown because they are Westinghouse Proprietary Information.)

Parameter	Value
Storage Cell Center-to-Center Pitch	9.028
Storage Cell Inner Dimension (Width)	8.8
Inter-Cell Flux Trap Gap	N/A
Storage Cell Length	199.5
Storage Cell Wall Thickness	0.075
Neutron Absorber Material	Metamic
Neutron Absorber Length	172
Neutron Absorber Width	7.5
Neutron Absorber Thickness	0.106
Distance from Top of Rack Baseplate to Bottom of Neutron Absorber	6.23
Neutron Absorber B_4C Loading	31 weight-percent
Neutron Absorber Sheathing Thickness Internal Walls Periphery Walls	 0.035 0.075
Baseplate Thickness	0.75
Baseplate Flow Hole Diameter	6
Rack Pedestal Type (fixed or adjustable)	Adjustable
Rack Pedestal Height (female + male)	2.75
Rack Female Pedestal Dimensions	18 x 18 x 2.25
Rack Male Pedestal Diameter	4.5
Rack Bearing Pad Thickness	1.5

ANNEXURE 2

This annexure provides a description of region 2 which was modelled in this study. This annexure was interpreted in order to build the model used.

2.4.1.2 KENO Model for Region 2 "All-Cell" Storage Configuration

The Region 2 "All-Cell" fuel assembly storage configuration is modeled in KENO as a 12x12 array of "stainless steel canister" storage cells and "developed" storage cells. The pitch modeled between storage cells is 9.028 inches.

The KENO model for a 12x12 array of Region 2 storage cells was developed to accurately represent the construction of these storage cells. Note that the largest Region 2 module is a 12x11 array of storage cells. Therefore, the KENO results for a 12x12 array of storage cells (with periodic boundary conditions) will bound the expected results for the largest Region 2 module.

The fuel assembly inside each storage cell is a depleted Westinghouse AP1000 17x17 assembly. The stainless steel canister is modeled with an inside dimension of 8.8 inches and is 0.075 inch thick. Metamic poison panels are modeled as attached to the outside of the stainless steel canister. The Metamic panels are modeled as 7.5 inches wide and 0.106 inch thick. Stainless steel sheathing panels hold the Metamic panels in place and are modeled as 0.035 inch thick. Note that there is a small gap between the Metamic poison panels and the stainless steel sheathing that is modeled as a void 0.012 inches thick. The Metamic poison material is modeled with the minimum B-10 areal loading. The stainless steel canister, fuel assembly, Metamic panels, and stainless steel sheathing are all modeled as 168 inches tall and are elevated above the concrete floor by 13.23 inches.

A 2-foot water reflector is modeled above each storage cell, and a 13.23-inch water reflector is modeled below each storage cell. Reflective boundary conditions are applied to the top of the top water reflector and bottom of the bottom water reflectors respectively. Periodic boundary conditions are applied on the lateral surfaces of the 12x12 array. This simulates an infinitely repeating 12x12 array of storage cells. The pool water is simulated to be full density (1 $g/cm^{3)}$ at room temperature (20°C).

2.3.3.2 Region 2 Storage Cell Description

The Region 2 storage cells are formed by welding open stainless steel canisters together at the corners. Therefore, the Region 2 storage cells are a combination of individual canister storage cells and "developed" storage cells. The "developed" storage cells result from the welding process. As an example, the welding of four canisters at the corners of each canister produces a single "developed" storage cell at the center of the four canisters. Each Region 2 stainless steel canister has an inside dimension of 8.8 inches and is 0.075 inch thick. The center-to-center spacing between storage cells is 9.028 inches.

Metamic panels are attached to the outside surfaces of each stainless steel canister except for the surfaces directly facing the walls of the spent fuel pool. Each Metamic poison panel is held in place and is centered on the surface of the stainless steel canister by an outer stainless steel sheathing panel. There is a small void space (0.012 inch) between the sheathing and the Metamic panel. The dimensions of the Metamic poison panel are 7.5 inches wide by 0.106 inch thick. The sheathing panels on interior storage canisters are 0.035 inch thick.

Each Region 2 storage cell is 199.5 inches long and rests on top of a base plate whose top is 5 inches above the concrete floor. Note that each Metamic poison panel is 172 inches long and has a bottom elevation that is 6.23 inches above the top of the base plate. The bottom elevation of the Metamic poison panel was positioned to be 2 inches lower than the bottom elevation of the active fuel. The Metamic poison material used in the Region 2 storage cells is a mixture of B_4C and Al with a nominal B_4C concentration equal to 31.0 weight-percent, and uses natural Boron isotopics (i.e., not enriched B^{10}). The Region 2 storage cell dimensions are summarized in Table 2-6.

ANNEXURE 3

This annexure provides Table 2-11 from the COLA document. This table was used as a reference for the model that was built in this study.

Table 2-11 K_{eff} Values for the Tolerance/Uncertainty Cases for the Region 2 "All-Cell" Storage Configuration

Case Description	K_{eff}	ΔK_{eff}
Nominal Case[1]	0.97064 ± 0.00051	N/A
Increase in U-235 Enrichment (+0.05 weight-percent)	0.97840 ± 0.00053	0.00880
Increase in UO_2 Density (+1%)	0.97216 ± 0.00048	0.00251
Increase in Pellet OD (+0.0005 in.)	0.97239 ± 0.00049	0.00275
Decrease in Clad OD (-0.0015 in.)	0.97266 ± 0.00048	0.00301
Decrease in Cell Pitch (-0.04 in.)	0.97184 ± 0.00049	0.00220
Increase in Cell Wall Thickness (+0.007 in.)	0.97135 ± 0.00056	0.00178
Decrease in Cell ID (-0.04 in.)	0.97069 ± 0.00052	0.00108
Increase in Sheathing Thickness (+0.004 in.)	0.97219 ± 0.00054	0.00260
Decrease in Metamic Width (-0.0625 in.)	0.97289 ± 0.00053	0.00329
Asymmetric Assembly Positioning	0.96833 ± 0.00056	-0.00124 (set to zero)
Burnup Uncertainty[2]		0.00941
Methodology Uncertainty[3]		0.00657
Statistical Sum of Uncertainties		0.01609
Methodology Bias[4]		0.00310
Temperature Bias[5]		0.0 (Negative)
Sum of Uncertainties and Biases		**0.01919**

Notes:

1. The nominal case for the Region 2 "All-Cell" storage configuration contains standard fuel assembly at the fresh enrichment of 2.07 weight-percent U-235.
2. Burnup uncertainty is found by evaluating the differential burnup worth at the conservative maximum burnup credit value of 35,000 MWD/MTU.
3. Methodology uncertainty is the statistical sum of the methodology calculational variance and the KENO uncertainty, using a maximum KENO uncertainty of all the bias and uncertainty calculations for this configuration equal to 0.00080.
4. Methodology bias or the mean calculational methods bias is evaluated to be 0.00310 (see subsection 2.2.1 for background).
5. Pool temperature bias is calculated with the 238-group library at a burnup equal to 25,000 MWD/MTU and an initial enrichment equal to 4.0 weight-percent U-235.